2018

B1 Cell IgE Impedes Mast Cell-Mediated Enhancement of Parasite Expulsion through B2 IgE Blockade

Rebecca K. Martin
Virginia Commonwealth University

Sheela R. Damle
Virginia Commonwealth University

Yolander A. Valentine
Virginia Commonwealth University

See next page for additional authors

Authors

Rebecca K. Martin, Sheela R. Damle, Yolander A. Valentine, Matthew P. Zellner, Briana N. James, Joseph C. Lownik, Andrea J. Luker, Elijah H. Davis, Martha M. DeMeules, Laura M. Khandjian, Fred D. Finkelman, Joseph F. Urban Jr., and Daniel H. Conrad

B1 Cell IgE Impedes Mast Cell-Mediated Enhancement of Parasite Expulsion through B2 IgE Blockade

Graphical Abstract
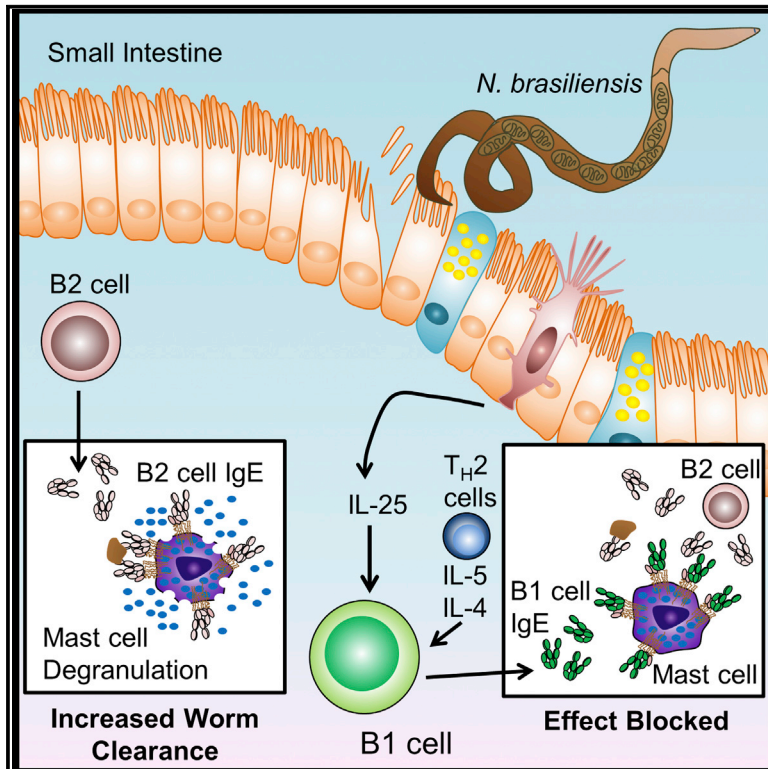
Authors

Rebecca K. Martin, Sheela R. Damle, Yolander A. Valentine, ..., Fred D. Finkelman, Joseph F. Urban, Jr., Daniel H. Conrad

Correspondence

daniel.conrad@vcuhealth.org

In Brief

Martin et al. show that B1 cell IgE is induced during Th2 helminth infections by IL-25. This B1 cell IgE blocks parasite clearance through inhibition of mucosal mast cell activation by B2 cell IgE.

Highlights

- B1 cells make IgE in response to helminths

- IL-25 induces B1 cell IgE production in cells harvested from helminth-infected mice

- B2 cell IgE enhances helminth clearance in a mast cell-dependent manner

- B1 cell IgE blocks B2 cell-mediated helminth clearance

B1 Cell IgE Impedes Mast Cell-Mediated Enhancement of Parasite Expulsion through B2 IgE Blockade

Rebecca K. Martin,[1,7] Sheela R. Damle,[1,7] Yolander A. Valentine,[1] Matthew P. Zellner,[1] Briana N. James,[1] Joseph C. Lownik,[1,2] Andrea J. Luker,[1] Elijah H. Davis,[1] Martha M. DeMeules,[1,3] Laura M. Khandjian,[1] Fred D. Finkelman,[4,5] Joseph F. Urban, Jr.,[6] and Daniel H. Conrad[1,8,*]

[1]Department of Microbiology and Immunology, School of Medicine, Virginia Commonwealth University, Richmond, VA 23298, USA
[2]Center for Clinical and Translational Research, School of Medicine, Virginia Commonwealth University, Richmond, VA 23298, USA
[3]University of Wisconsin-Madison, Madison, WI 53715, USA
[4]Division of Immunology, Department of Internal Medicine, University of Cincinnati College of Medicine, Cincinnati, OH 45267, USA
[5]Medicine Service, Veterans Administration Medical Center, Cincinnati, OH, USA
[6]United States Department of Agriculture, Agricultural Research Service, Diet, Genomics and Immunology Laboratory, Beltsville, MD 20705, USA
[7]These authors contributed equally
[8]Lead Contact
*Correspondence: daniel.conrad@vcuhealth.org
https://doi.org/10.1016/j.celrep.2018.01.048

SUMMARY

Helminth infection is known for generating large amounts of poly-specific IgE. Here we demonstrate that innate-like B1 cells are responsible for this IgE production during infection with the nematode parasites *Nippostrongylus brasiliensis* and *Heligmosomoides polygyrus bakeri*. *In vitro* analysis of B1 cell immunoglobulin class switch recombination to IgE demonstrated a requirement for anti-CD40 and IL-4 that was further enhanced when IL-5 was added or when the B1 source was helminth infected mice. An IL-25-induced upregulation of IgE in B1 cells was also demonstrated. In T cell-reconstituted RAG1$^{-/-}$ mice, *N. brasiliensis* clearance was enhanced with the addition of B2 cells in an IgE-dependent manner. This enhanced clearance was impeded by reconstitution with IgE sufficient B1 cells. Mucosal mast cells mediated the B2 cell enhancement of clearance in the absence of B1 cells. The data support B1 cell IgE secretion as a regulatory response exploited by the helminth.

INTRODUCTION

Immunoglobulin E (IgE) is an evolutionarily conserved immunoglobulin that is well known for causing the symptoms of atopic disease. This antibody class, despite having a half-life of less than a day in plasma, can persist for weeks to months when bound to cell surface FcεRI, making it a long-lasting "gatekeeper" particularly with respect to triggering mast cells (MCs) or basophils (Oettgen, 2016). Specific IgE responses directed against innocuous particles, such as pollen, cat dander, or peanut proteins, can result in allergic disease. IgE-mediated responses range from mild to severe. They can be either site directed, such as allergic rhinitis, atopic dermatitis, urticaria, and asthma, or systemic, as in anaphylactic shock. IgE$^+$ plasma cells generated in the germinal centers (GCs) that produce high-affinity IgE to antigens are purported to come from bone marrow (BM)-derived B cells or B2 cells through immunoglobulin class switch recombination (CSR) and somatic hyper mutation (SHM). In contrast, memory IgE responses are generated from IgG1$^+$ memory B cells (Oettgen, 2016).

B1 cells develop early in ontogeny, prior to the first hematopoietic stem cell (HSC), and are derived initially from the fetal yolk sac and then from the fetal liver (Savage and Baumgarth, 2015). They are delineated from B2 cells by the expression of CD11b and absence of CD23. They reside primarily in the pleural and peritoneal body cavities of mice and traffic to the draining lymph nodes (LNs), spleen, and mucosal sites upon activation (Yenson and Baumgarth, 2014; Savage and Baumgarth, 2015; Waffarn et al., 2015). B1 cells are important immune effectors and regulators of adaptive immunity that bridge the innate and adaptive immune systems. The B cell receptor (BCR) repertoire in these cells is enriched for poly-specific receptors encoded in the germline with low affinities to a broad range of antigens (Baumgarth et al., 2005). B1 cells are essential Immunoglobulin M (IgM) secretors and have additionally been shown to be the definitive source of "natural" IgM. As immune effectors, they also secrete Immunoglobulin A (IgA) at mucosal sites. However, only a few reports have demonstrated IgE production by B1 cells (Takatsu et al., 1992; Vink et al., 1999; Perona-Wright et al., 2008; Savage and Baumgarth, 2015). The importance of parasite-specific IgE in controlling infection is controversial, yet there is evidence to support IgE-mediated clearance of phylogenetically distinct helminths such as *Schistosoma mansoni* and *Trichnelia spiralis* (Joseph et al., 1983; Gurish et al., 2004; Oettgen, 2016). These parasites strongly promote IgE synthesis (Wu and Zarrin, 2014). In this work, we showed that poly-specific IgE made by B1 cells was responsible for reduced MC degranulation by mechanism of IgE saturation of FcεRI that was initially proposed by Bazaral et al. (1973).

Nippostrongylus brasiliensis and *Heligmosomoides polygyrus bakeri* are Th2-inducing helminth parasites of mice similar to the human hookworms, *Necator americanus* and *Ancylostoma*
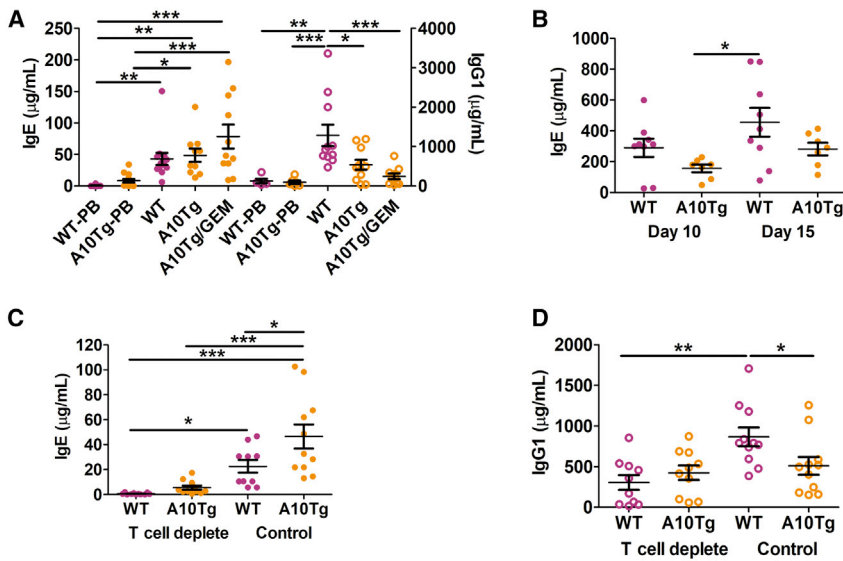
Figure 1. B1 Cell IgE Is Induced with T Cell Help during Helminth Infection

(A–D) Total serum IgE (closed circles) (A and C) and IgG1 (open circles) (A and D) was measured on day 0 (PB) and 14 post *N. brasiliensis* inoculation in ADAM10Tg (A10Tg, orange) and wild-type (WT; magenta) mice. Where indicated, GEM depletion of MDSCs was performed.

(B) Total serum IgE was measured on days 10 and 15 post *H. polygyrus bakeri* inoculation.

(C and D) Mice were T cell depleted or treated with control IgG mAb followed by *N. brasiliensis* infection. *p < 0.05, **p < 0.01, ***p < 0.001. If not indicated, the comparison was not significant between groups. The error bars depict SEM. (A) was representative of three independent experiments. (B), (C), and (D) were representative of two independent experiments. One-way ANOVA with a Tukey post hoc was used to compare all IgE or all IgG1 groups in (A)–(D).

duodenale (de Silva et al., 2003). Wild-type (WT) mice are able to clear these infections in a T cell-dependent manner, relying on the cytokines IL-13 and IL-4 for the "weep and sweep" of intestinal helminth clearance (Madden et al., 2002; Finkelman et al., 2004). This refers to the increased mucus production, goblet cell hyperplasia, and enteric nerve stimulation associated with intestinal parasite expulsion(Camberis et al., 2003; Finkelman et al., 2004). In response to these intestinal helminths, we demonstrated that B1 cells class switch to IgE. In addition, the signals that drive B1 cells to IgE production and the functional relevance of B1 cell IgE in parasite-host interactions are shown.

RESULTS

B1 Cells Make Large Amounts of IgE in Response to Helminth Infection

In our laboratory, we generated mice that lack BM-derived B cells, or B2 cells (Gibb et al., 2011), the ADAM10Tg mouse. This is due to overexpression of ADAM10 at the common lymphoid progenitor stage that leads to improper NOTCH signaling and loss of B cell development. As this defect is restricted to the BM, the B1 cell compartment is intact (Gibb et al., 2011). To study the B1 cell antibody response during helminth infection, we inoculated ADAM10Tg and WT control mice with *N. brasiliensis* or *H. polygyrus bakeri* infective third-stage larvae (L3). We measured the amount of IgE and Immunoglobulin G1 (IgG1) antibody in the serum in the naive state and on day 14 post infection. Interestingly, there was no significant difference in IgE production between WT and ADAM10Tg mice infected with either helminth (Figures 1A and 1B). This suggested that B1 cells produced significant levels of IgE post helminth infection in the absence of B2 cells. ADAM10Tg mice have an increased number of immature myeloid cells throughout the organs and circulation due to the defect in hematopoiesis (Gibb et al., 2011). These cells were selectively depleted utilizing gemcitabine (GEM) to assess whether they played a role in enhancing B1 cell IgE (Sinha et al., 2007; Saleem et al., 2012). *N. brasiliensis*-infected and GEM-

treated mice exhibited no change in IgE levels (Figure 1A), indicating an inconsequential role of immature myeloid cells on B1 cell IgE antibody production. Myeloid-derived suppressor cell (MDSC) depletion was confirmed by flow cytometry (Figure S1A). To ensure B1 IgE production was not altered due to ADAM10 overexpression, we sorted B1 cells (Figure S1B), and ADAM10 message was not different, as measured by qPCR (Figure S1C).

B1 Cell IgE Production during Helminth Is T Cell Dependent

To assess whether helminth-induced B1 cell IgE production required T cells, we depleted both CD8+ and CD4+ T cells with GK1.5 and 2.43 antibodies, respectively (Saleem et al., 2012). Both WT and ADAM10Tg mice had significantly reduced IgE production after T cell depletion (Figure 1C). WT mice had significantly reduced IgG1 after T cell depletion that was not seen in ADAM10Tg mice (Figure 1D). IgG1 levels were significantly reduced in ADAM10Tg mice (Figures 1A and 1D). The reason for this is not known; however, the ADAM10Tg mice make IgE that is equivalent or more than WT levels (Figures 1A and 1C). A baseline level of IgE and IgG1 remained in both WT and ADAM10Tg mice despite the loss of T cells (Figures 1C and 1D). This could represent a small amount of T cell-independent IgE production.

B1 Cell Antibody Production after NP-KLH Immunization Is Not NP Specific

We next examined the antigen specificity of B1 cell IgG1 in the ADAM10Tg mouse. Mice were immunized intraperitoneally (i.p.) with NP$_{32}$-KLH in alum and both high-affinity IgG1 antibody and total specific IgG1 antibody was assessed in serum by enzyme-linked immunosorbent assay (ELISA) (Smith et al., 1997). On day 14, ADAM10Tg mice have almost undetectable nitrophenol (NP)-specific IgG1 antibody (Figures 2A and 2B) in addition to having measurable total IgG1 that was significantly less than WT (Figure 2C). A boost at day 28 induced increased
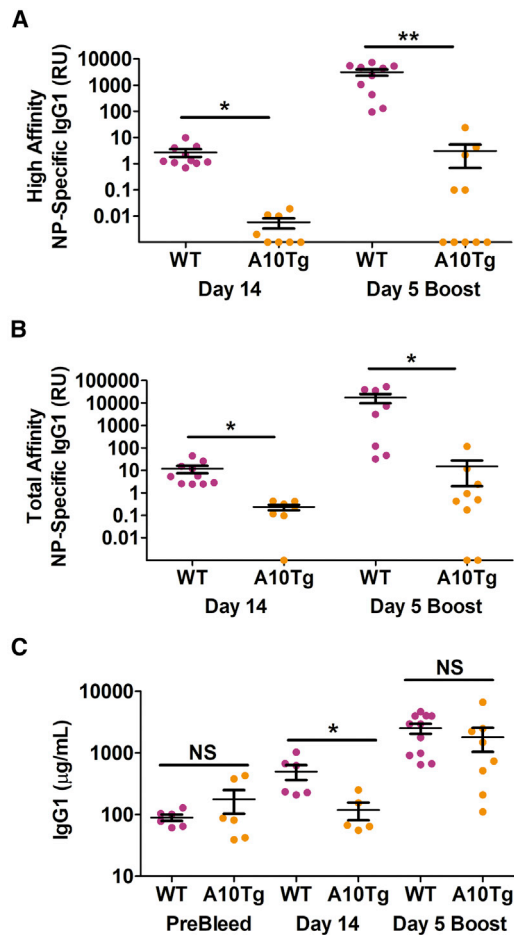
Figure 2. B1 Cell Antibody Responses to NP-KLH Are Not Specific
(A–C) ADAM10Tg (A10Tg, orange) and WT (magenta) mice were immunized i.p. with NP_{32}-KLH in alum. Serum levels of high-affinity NP-specific (NP_4BSA-binding) (A), total NP-specific IgG1 ($NP_{25}BSA$ binding) (B), and total IgG1 (C) were measured by ELISA on day 0, 14, and day 5 post boost. NS, not significant; *p < 0.05, **p < 0.01. The error bars depict SEM. Significance was obtained using an unpaired Student's t test to compare WT and A10Tg. Data are from three independent experiments.

high-affinity IgG1, total specific IgG1, and total IgG1 in WT mice (Figures 2A–2C). ADAM10Tg mice, while having a large spread in total IgG1, did not increase significantly after the boost, even from the naive bleed (Figure 2C), and though some animals developed a limited amount of NP-specific IgG1, it was three to four orders of magnitude different than the WT (Figures 2A and 2B).

B1 Cell-Derived IgE Fails to Induce MC Degranulation

A major function of antigen-specific IgE is to induce degranulation through FcεRI on MCs and basophils. To measure the antigen specificity of B1 cell IgE as well as examine the ability of B1 cell antibody to induce degranulation, we used a model of active cutaneous anaphylaxis (ACA) (Evans et al., 2014). MC degranulation was induced by crosslinking OVA-specific IgE molecules bound to FcεRI on skin MCs; the resulting dye leakage creates

a blue spot. This degranulation can also result from and be enhanced by IgG complexes bound to FcγRIII (Strait et al., 2006). Measurement of the area of the spot and its content of Evans blue in WT mice indicated significantly increased MC degranulation compared to ADAM10Tg mice (Figures 3A and 3B) despite an equivalent total IgE (Figure 3C) and IgG1 (Figure 3D) in the serum of both groups of mice. This indicated that neither the B1 cell IgE nor the B1 cell IgG1 induced with this antigen in alum was OVA specific. Further, OVA-specific IgE was confirmed as significantly less by ELISA in the ADAM10Tg mice (Figure 3E). Next, blocking of specific IgE to FcεRI by helminth-induced B1 cell antibody was tested in a model of passive cutaneous anaphylaxis (PCA). ADAM10Tg and WT mice were infected with *N. brasiliensis* L3, and PCA reaction was assessed 21 days later (Figures 3F and 3G). All uninfected control mice had no statistical differences in degranulation, indicating that skin MC activation was normal (Figures 3F and 3G). Additionally, numbers of MCs in the skin between ADAM10Tg and WT mice were equivalent (data not shown), but the amount of MC degranulation seen in both ADAM10Tg and WT mice was significantly reduced by helminth infection (Figures 3F and 3G) supporting a helminth-induced blockage of MC degranulation. Total IgE levels in these mice were equivalent and increased during helminth infection (Figure 3H). Total IgG1 levels were elevated in WT mice after helminth infection, but not in ADAM10Tg mice (Figure 3I). This is similarly seen in previous infections (Figures 1A and 1C). To illustrate that this PCA suppression was IgE dependent, we utilized IgE deficient mice ($IgE^{-/-}$). After *N. brasiliensis* infection, there was no evidence of suppression of the PCA reaction in $IgE^{-/-}$ mice (Figures 3F and 3G).

B1 Cells Are Primed to Make IgE during Helminth Infection

To investigate the signals necessary for the B1 cell to class switch to IgE, we sorted peritoneal cavity B1 from naive or *N. brasiliensis*-infected mice (Figure S1B). Naive B1 cells make little IgE when treated with anti-CD40 and IL-4, but the addition of IL-5, a known B1 proliferative agent (Erickson et al., 2001; Takatsu, 2011), significantly increased IgE production (Figure 4A). Interestingly, B1 cells from *N. brasiliensis*-infected mice made significantly more IgE than from B1 cells from naive mice, after anti-CD40 and IL-4 treatment. This did not correlate with increased cell proliferation (Figures 4 A and 4B). When IL-5 was added, B1 cells from *N. brasiliensis*-infected mice had increased sensitivity to IL-5-induced proliferation, and this correlated to increased IgE production as well (Figures 4 A and 4B). Overall, this indicated that B1 cell IgE was stimulated *in vitro* by similar signals as B2 cell-induced IgE with respect to anti-CD40 and IL-4; however, other signals may be priming B1 cells for increased IgE production during infection with *N. brasiliensis*. Since B1 cells are known to secrete large amounts of IgM, IgM production by both B1 and B2 cells was compared in culture. B1 cells from *N. brasiliensis*-infected mice treated with anti-CD40, IL-4, and ± IL-5 made significantly more IgM than similarly treated B2 cells from infected mice, reinforcing that B1 cells were being examined (Figure S2A).
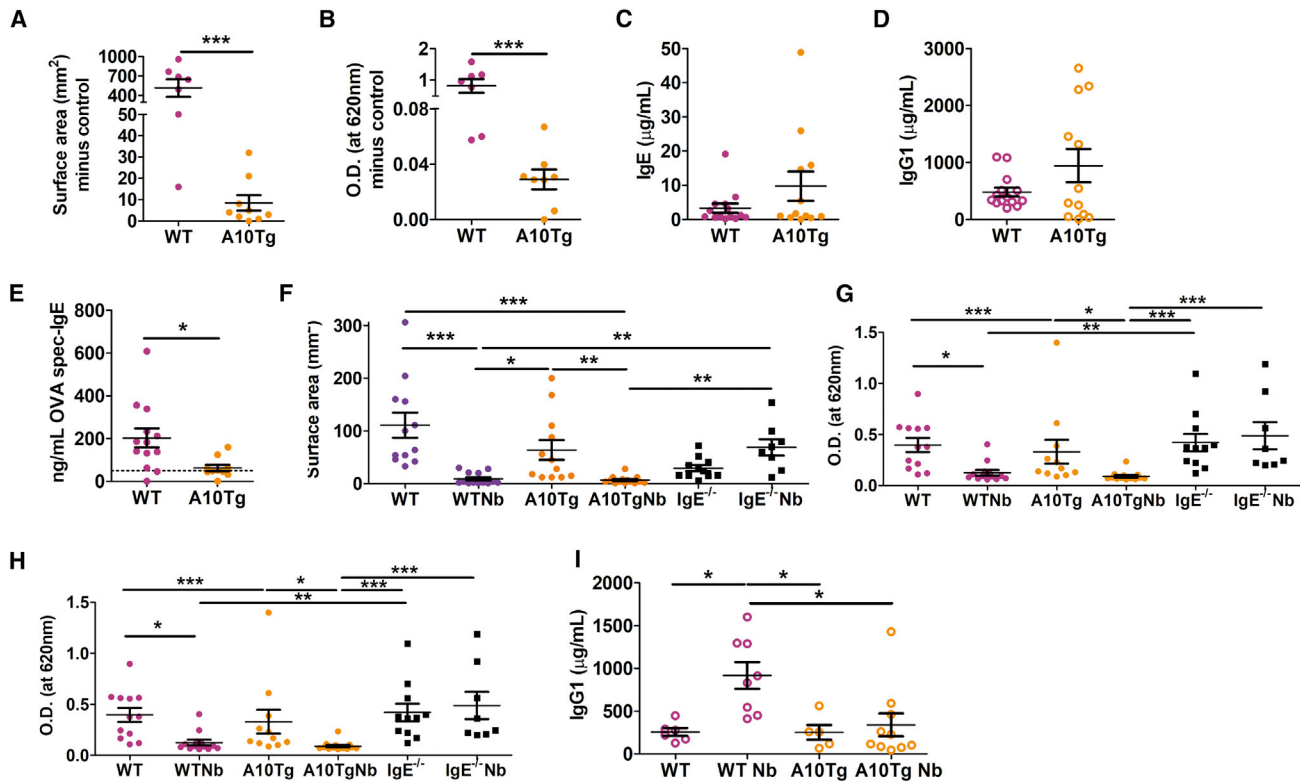
Figure 3. Antibody Produced by B1 Cells Blocks Antigen-Specific IgE-Mediated MC Degranulation

(A–E) ADAM10Tg (A10Tg, orange) and WT (magenta) mice were immunized with OVA in alum for an ACA model. Post i.d. OVA challenge and i.v. injection with Evan's blue dye solution, MC degranulation was measured by dye release into the back skin as surface area of the spot (A) and dye extraction (B) (minus control spot). Total serum IgE (C), serum IgG1 (D), and OVA-specific IgE (E) (dotted line depicts limits of detection) antibody were as measured from sera just prior to ACA test. PCA model utilized either naive or day 21 post-*N. brasiliensis* (Nb) mice.

(F and G) Surface area of the spot (F) or dye extraction (G) was measured in WT, A10Tg, or IgE deficient (IgE$^{-/-}$) mice.

(H and I) Total serum IgE (H) and serum IgG1 (I) antibody were measured from sera collected just prior to PCA test.

*p < 0.05, **p < 0.01, ***p < 0.001. If not indicated, the comparison was not significant between groups. Error bars depict SEM. Significance was obtained as follows: Student's t test for (A)–(E), Kruskal-Wallis test with a Dunn's multiple comparison for (F) and (G), and a one-way ANOVA with a Tukey post hoc test for (H) and (I).

The Alarmin IL-25, but Not IL-33, Enhances B1 Cell IgE Production during Helminth Infection

IL-25 production by intestinal tuft cells has been shown to be important for cytokine production by ILC2 and Th2 cells (von Moltke et al., 2016; Gerbe et al., 2016). Fort et al. (2001) reported that i.p. IL-25 injection induced IgE production at 10 days. These data, as well as the importance of IL-25 release by intestinal tuft cells during helminth infection, led to an examination of the effects of IL-25 on B1 cell IgE. B1 cells from *N. brasiliensis*-infected mice, but not naive mice, made significantly more IgE when treated with anti-CD40, IL-4, and IL-25 (in the range of 1 to 100 ng/mL) as compared to cells treated with anti-CD40 and IL-4 alone (Figures 5A and 5B). IL-25 plus IL-5 did not further increase B1 cell IgE production from either naive or *N. brasiliensis*-infected B1 cells (Figures 5A and 5C). In addition, IL-25 induced a moderate amount of proliferation in B1 cells treated with anti-CD40 and IL-4 (Figure 5D), but the increased baseline proliferation seen with IL-5, anti-CD40, and IL-4 treated B1 cells was not further augmented with

IL-25 (Figure 5E). The increase in IgE seen after treatment with IL-25 in B1 cells from *N. brasiliensis*-infected mice was demonstrated by quantitative RT-PCR (qRT-PCR) analysis of secreted IgE expression (Figure 5F). Additional controls show that IL-25 alone did not induce detectable levels of IgE in culture (Figures S2G–S2I).

Since IgM is typically secreted by B1 cells, the regulation of IgM levels by IL-25 was examined. B1 cells from naive mice treated with anti-CD40 and IL-4 produced IgM that was not affected by the addition of IL-25, with or without IL-5 (Figures S2B and S2C). IL-5 increased IgM production overall (Figures S2B and S2C). Inversely, B1 cells from mice infected with *N. brasiliensis* that were treated with anti-CD40 and IL-4 had lower IgM when treated with IL-25 compared to naive. IL-25 also had no significant effect on IgG1 levels by ELISA (Figures S2D and S2E) or qRT-PCR (Figure S2F). To see whether this pathway was active only in B1 cells, we examined IgE production in B2 cells from both naive and *N. brasiliensis*-infected mice. IgE, IgG1, and IgM were not significantly altered beyond the addition

A

B
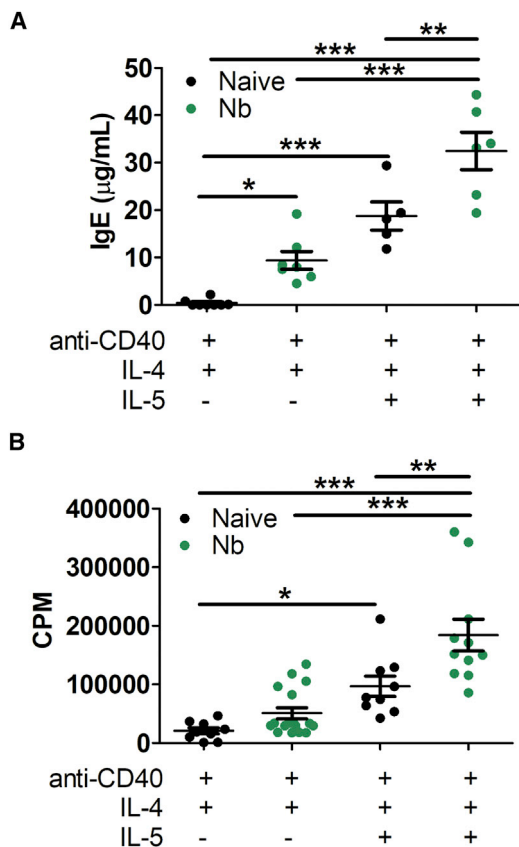
Figure 4. IL-5 Enhanced IgE Production in B1 Cells

B1 cells were sorted (CD23$^-$B220^{int}, CD11b^{int}, CD138$^-$) (Figure S1B shows gating) from the peritoneal lavage of mice infected with *N. brasiliensis* (day 14) or naive WT mice.

(A) 30,000 cells/mL were cultured with anti-CD40, IL-4, ± IL-5. Supernatants were harvested on day 9 of culture for total IgE ELISA.

(B) For proliferation, 60,000 cells/mL were cultured for 72 hr, followed by the addition of 1 μCi/well [H^3]-thymidine with cell harvest at 24 hr later.

CPM, counts per minute. *p < 0.05, **p < 0.01, ***p < 0.001. Error bars depict SEM. Significance was obtained using a one-way ANOVA with a Tukey post hoc test.

of anti-CD40 and IL-4 (Figures S3A–S3F). In addition, IL-25 alone did not induce IgE, IgG1, or IgM secretion by B2 cells (Figures S3A–S3F).

Komai-Koma et al. recently showed that B1 cells proliferate after daily i.p. injection with IL-33 (Komai-Koma et al., 2011) through production of IL-5 that then upregulated ST2 on B1 cells (Ahmed and Koma, 2015). To test the effect of IL-33 on B1 cell IgE production, we injected IL-33 i.p. into WT mice and compared sorted B1 cells to B1 cells from naive mice. IL-33 injected i.p. did not increase B1 cell IgE or IgG1 (Figures S4D and S4E). In addition, *in vitro* IL-33 treatment also failed to increase IgE or IgG1 production, either with or without IL-5 pretreatment (Figures S4D and S4E). Finally, *ex vivo* IL-33 treatment did not enhance IgE secretion by B1 cells isolated from mice infected with *N. brasiliensis* but did increase proliferation, as described (Figures S4A–S4C). These data suggest that IL-33 does not enhance IgE production in B1 cells.

IL-25-Dependent B1 Cell-Produced IgE Blocks Enhanced B2 Cell-Produced IgE-Mediated Suppression of *N. brasiliensis*

To examine the physiological importance of B1 cell-produced IgE during infection with *N. brasiliensis*, we turned to a RAG1$^{-/-}$ mouse model that lacks functional T cells and B cells, including B1 cells (Paciorkowski et al., 2000). All mice were reconstituted with WT CD4$^+$ T cells and further reconstituted with B1 cells alone, B2 cells alone, or B1 and B2 cells. One week after reconstitution, mice were inoculated with *N. brasiliensis* L3. The total number of lymphocytes that are reconstituted after 1 week was determined by flow cytometry and compared to that of a WT mouse (Figures S5A–S5F). Proper reconstitution was confirmed by flow cytometry after *N. brasiliensis* infection (Figure S5G). The level of infection was monitored by measuring fecal egg levels (Figures 6A and 6B). Both B1 cell-only and CD4$^+$ T cell-control reconstituted mice had similar infection levels, demonstrating that B1 cells did not alter parasitic clearance mediated directly by CD4$^+$ T cells (Figures 6A and 6B). Intriguingly, B2 cell-only reconstituted mice showed significantly decreased egg production compared to the other groups, and B1/B2 cell-reconstituted mice showed greater egg production compared to the B2 cell-only group (Figures 6A and 6B). This indicated that B1 cells were hindering B2-mediated clearance. To test whether this was B1 cell IgE mediated, we reconstituted mice with B1 cells from IgE$^{-/-}$ mice and WT B2 cells. These IgE$^{-/-}$ B1 cells did not inhibit the B2-mediated suppression of egg production (Figures 6A and 6B). To further show that the B2-mediated suppression of egg production was IgE dependent, we reconstituted RAG1$^{-/-}$ mice with IgE$^{-/-}$ B2 cells. These B2-IgE$^{-/-}$ mice exhibited considerably greater egg production than the mice reconstituted with WT B2 cells (Figures 6A and 6B). The total IgE levels in serum were similar between all three groups that had been reconstituted with WT B cells and were only significantly reduced in the IgE$^{-/-}$ mice (Figure 6C).

These mice were maintained for 35 days after *N. brasiliensis* inoculation and then injected intradermally (i.d.) with *N. brasiliensis* excretory-secretory extract (NES) in a model of ACA to determine whether B1 cell IgE provided protection against IgE-mediated helminth-specific MC degranulation. We observed that the mice reconstituted with WT B2 cells generated an ACA reaction (Figures 6D and 6E). The mice that were reconstituted with WT B1 and WT B2 had reduced ACA responses reflective of their decreased parasite clearance (Figures 6D and 6E). Mice reconstituted with IgE$^{-/-}$ B2 cells from *N. brasiliensis*-infected mice failed to induce ACA responses. Mice that had been reconstituted with both IgE$^{-/-}$ B1 cells and WT B2 cells generated ACA skin reactions similar to WT B2 cells alone, demonstrating the importance of B1 cell-derived IgE in blocking B2 cell induced degranulation (Figures 6D and 6E).

To examine whether this B1 cell-derived IgE was dependent on the cytokine IL-25, we reconstituted RAG1$^{-/-}$ mice with either WT B2 cells and WT B1 cells or WT B2 cells and B1 cells from IL-25 receptor deficient mice (IL-25R$^{-/-}$). These were both compared to mice with just WT B2 cells. As the IL-25R$^{-/-}$ mice were on a BALB/c background, this experiment used the BALB/c
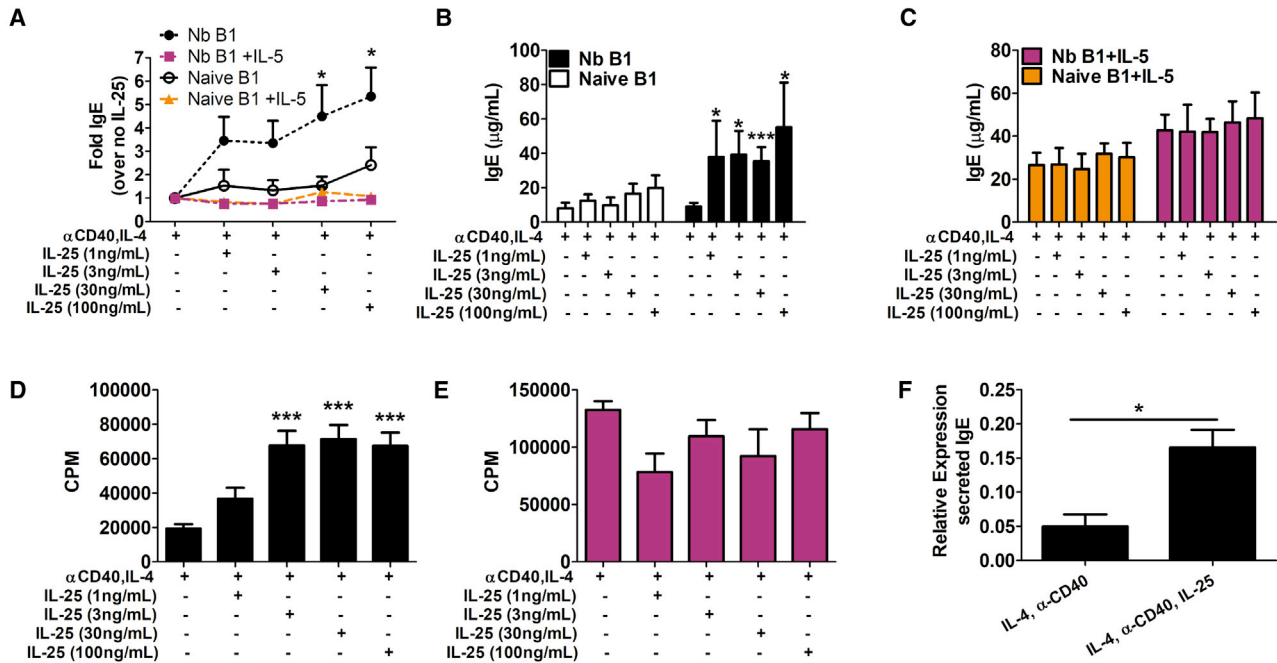
Figure 5. IL-25 Enhanced B1 Cell IgE Production Only from Helminth-Infected Mice

B1 cells were sorted (Figure S1B) from mice infected with *N. brasiliensis* or naive mice. They were then cultured with anti-CD40, IL-4, ± IL-5 and with increasing doses of IL-25.

(A) Fold change in IgE as compared to no IL-25 was assessed.

(B and C) Total IgE from no IL-5 in cultures (B) and IL-5 added to cultures (C).

(D and E) Proliferation of B1 cells from mice infected with *N. brasiliensis* was examined as in Figure 4 after addition of IL-25, without (D) or with (E) IL-5. CPM, counts per minute.

(A–F) Secreted *Ighe* message was assessed after 4 days anti-CD40 and IL-4 culture in B1 cells ± 30 μg IL-25 and normalized to *Actb* from *N. brasiliensis* infected mice. Statistics: fold change in B1 cells from naive (black open circle, solid line) was compared to fold change in *N. brasiliensis*-infected mice (Nb) (black filled circle, dotted line) by unpaired Student's t test (A); comparison was made between no IL-25 and dosages of IL-25 added to culture using an unpaired Student's t test (B and C) and a Mann-Whitney, non-parametric comparison (D–F).

*p < 0.05, ***p < 0.001. If not indicated, the comparison was not significant. n > 7 mice per group in (A)–(E), n = 3 pooled mouse samples per group in (F). Error bars depict SEM. Experiments are the products of at least two independent repeats for all groups.

RAG1$^{-/-}$ mice. IL-25R$^{-/-}$ B1 cells were unable to hinder the WT B2 cell-mediated clearance (Figures 6F and 6G), strongly supporting the *in vitro* cytokine data for IL-25 enhancement of B1 cell IgE production.

B2 Enhancement of Helminth Clearance Is MC Dependent

To further elucidate the mechanism behind B2 cell IgE enhancement of helminth clearance, we infected T cell plus B2 cell or T cell only control reconstituted RAG1$^{-/-}$ mice with *N. brasiliensis* L3. ELISAs showed significant increases in both MC-produced histamine and MC protease-1 (MCPT-1) in the mucus of the jejunum on day 7 in B2 cell reconstituted mice (Figures 7A and 7B). qRT-PCR analysis of total jejunal tissue demonstrated that B2 cell reconstitution significantly increased MC protease genes *Mcpt1*, *Mcpt2*, *Cpa3*, and *Cma1*, consistent with a role for MCs in suppression of *N. brasiliensis* egg production (Figure 7C; Table S1). Expression of the Th2-associated genes *Il4*, *Il5*, *Il13*, *Il6*, and *Il9* were similar between T cell only and T cell plus B2 cell reconstituted mice, indicating that differences in *Il4* and *Il13* are probably not

responsible for the reduced fecal egg burden in mice that had received B2 cells (Figure 7C; Table S1). In contrast, the mucus-related genes *Muc2*, *Muc3*, *Tff2*, and *Fcgbp* are significantly elevated by B2 cell reconstitution, pointing to a mechanism for the increased clearance (Figure 7C; Table S1). Differences in the expression of additional genes were also examined as well as for un-reconstituted RAG1$^{-/-}$ mice infected with *N. brasiliensis* L3, naive mice (Table S1), and lung at day 2 post helminth infection (Table S2). In the lung, no gene expression was altered by B2 cell reconstitution except *Ear11*, an eosinophil-related gene.

To confirm that the mechanism was MC dependent, we injected anti-ckit antibody (ACK.2) into T cell plus B2 cell or T cell only controls to deplete MCs (Brandt et al., 2003). ACK.2-treated mice lacked the B2 enhancement of helminth clearance that was seen in control Rat IgG isotype treated mice (Figure 7D). MC depletion was confirmed in jejunal intestinal sections by chloroacetate esterase staining (Figure 7E) and in peritoneal lavage (PL) on day 7 post inoculation by flow cytometry (Figure 7F). As ckit is an important marker on ILC2s and these cells are implicated in helminth clearance, we examined the
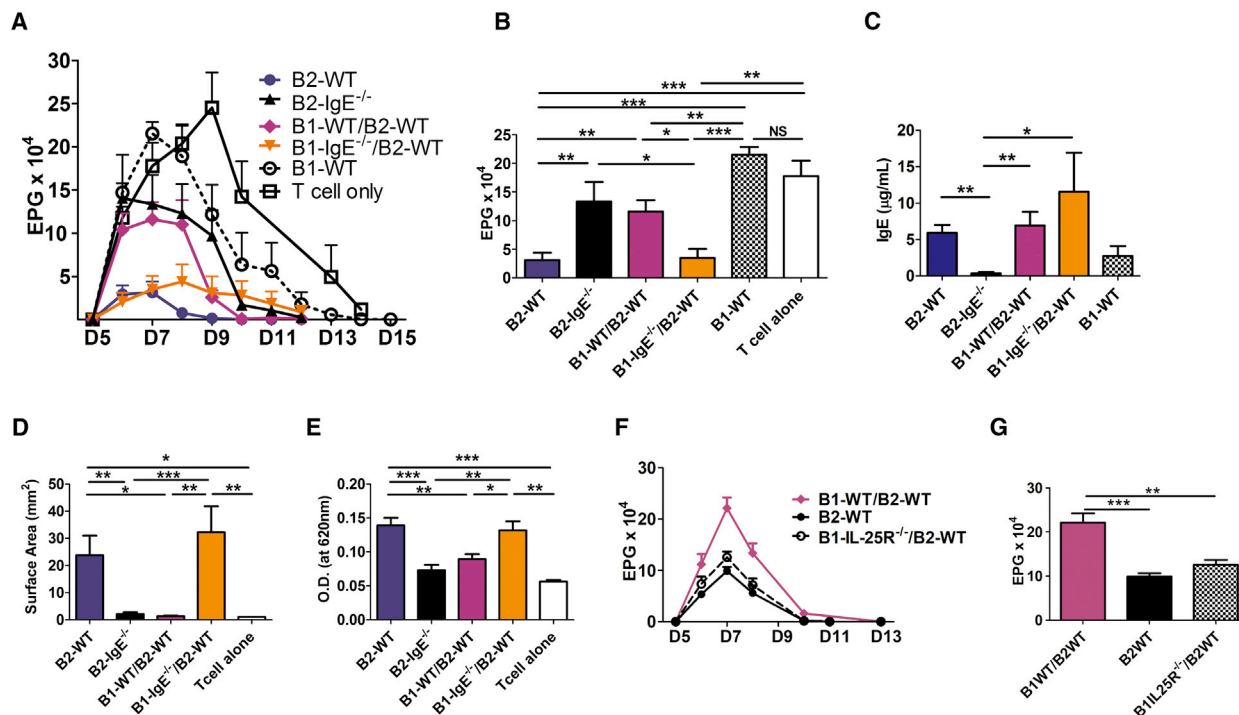
Figure 6. IL-25-Mediated B1 Cell IgE Blocks Parasite Clearance by B2 Cell IgE in Reconstituted Mice

RAG1$^{-/-}$ mice were reconstituted with the indicated cells as described in Experimental Procedures.

(A) Eggs per gram (EPG) of feces were determined over the time course of infection with *N. brasiliensis* L3.

(B) Day 7 EPG.

(C) Total serum IgE was measured in serum by ELISA on day 14.

(D and E) 35 days post infection, an ACA test was induced using NES and spot size (D) and dye extraction (E) from skin was assessed.

(F) EPG was measured over the time course of infection.

(G) Day 7 EPG.

*p < 0.05, **p < 0.01, ***p < 0.001. If not indicated, the comparison was not significant. For (A)–(E), n > 7 mice per group in all groups except T cell alone, which n = 4 mice per group and data are the product of four independent repeats. For (G) and (F), n = 4 mice per group, and data are representative of two independent repeats. Error bars depict SEM. Significance was determined as follows: one-way ANOVA with a Tukey post hoc for (B), (D), (E), and (G), and a Kruskal-Wallis non-parametric test with a Dunn's post hoc for (C).

mesenteric lymph node (MLN) and lung of ACK.2 and control RAG1$^{-/-}$ mice after *N. brasiliensis* infection for ILC2 percentage and numbers and found them not statistically different (Figures 7G, 7H, S5H, and S5I). To further support the IgE-mediated mechanism, we injected the anti-IgE antibody (R1E4, which blocks IgE binding to the FcεRI) i.p. into T cell plus B2 cell or T cell only controls to prevent IgE from binding to FcεRI (Baniyash et al., 1988). As in ACK.2-treated mice, R1E4-treated mice lacked the B2 enhancement of helminth clearance that was seen in the Rat IgG isotype control treated mice (Figures 7I and 7J).

To determine whether B1 cells suppressed antigen-specific IgG1 responses, we reconstituted RAG1$^{-/-}$ mice with CD4$^+$ T cells plus B1 and/or B2 cells and immunized them with NP$_{32}$-KLH in alum. RAG1$^{-/-}$ mice reconstituted with B1 cells only have significantly reduced total-specific and high-affinity IgG1 to the NP antigen, but NP-specific IgG1 levels and total IgG1 levels were similar in mice given B2 cells regardless of the addition of B1 cells. (Figure S5J). These data recapitulate the results observed in the ADAM10Tg mouse model.

DISCUSSION

B1 cells have long been thought to be important innate immune effectors. They generate critical IgM responses to bacteria, as well as to influenza virus (Savage and Baumgarth, 2015; Waffarn et al., 2015). In the past few years, a role for B1 cells in Th2 disease has emerged. Patel and Kearney (2015) demonstrated that B1 cell IgM blocked the response to a house dust mite (HDM) antigen asthma model, with germline anti-phosphorycholine (PC) antibody. Another study suggested that B1 cell IgE might be specific for PC in an HDM model, yet this was never shown (Patel and Kearney, 2015). Both *N. brasiliensis* and *H. polygyrus bakeri* have secreted PC epitopes (Péry et al., 1979; Hewitson et al., 2011). Recent studies have emphasized that B1 cell B cell receptors (BCRs) require stimulation during development without co-stimulation (Kreslavsky et al., 2017). Since this requires abundant amounts of antigen, the majority of B1 cell BCRs are self reactive (Kreslavsky et al., 2017). We do not know whether self-specific B1 cell IgE is present, but B1 cell IgE clearly does not enhance parasitic clearance (Figures 6A and 6B). In addition,
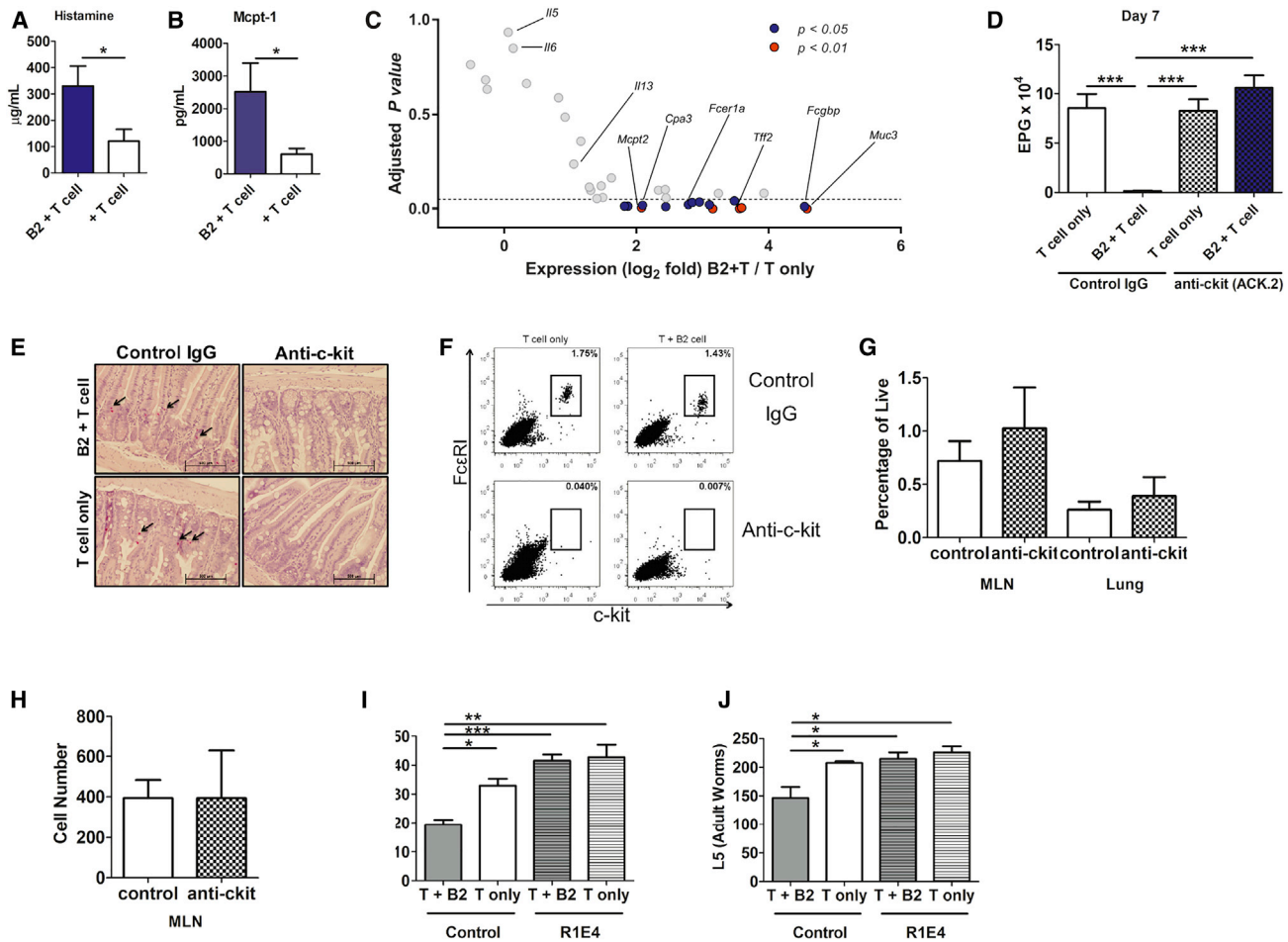
Figure 7. B2 Cell Enhanced Clearance Is MC and IgE Dependent

(A and B) Mice were reconstituted as in Figure 6. Day 7 post-*N. brasiliensis* infection. Histamine (A) and MCPT-1 (B) were measured by ELISA on mucus from the jejunum.

(C) Expression profiles from jejunal RNA were examined for genes potentially associated with helminth clearance (see also Tables S1 and S2).

(D) Mice were administered anti-ckit (ACK.2) antibody or control IgG daily starting at day 1 and day 7; EPG were measured.

(E) MCs were visualized in intestinal sections with chloroacetate esterase staining countered with hematoxylin (pink and arrows). Scale bar, 500 μm.

(F) PL was examined by flow for MCs (ckit$^+$FcεRI$^+$).

(G and H) MLN and lungs were examined by flow for ILC2 (Live,CD45$^+$Lin$^-$CD90.2$^+$Sca1$^+$ICOS$^+$) percentage (G) and number (H). (Gating schematic SF8A, B.) Reconstituted mice were infected with 750 *N. brasiliensis* L3 and treated with anti-IgE (R1E4) antibody or control IgG daily starting at reconstitution.

(I and J) On day 7, EPG (I) and adult worms (J) were measured.

*p < 0.05, **p < 0.01, ***p < 0.001. n > 8 mice per group in (A), (B), and (D)–(F). n = 6 mice per group in (C). n = 3 mice per group in (G) and (H). n = 4 mice per group in (I) and (J). Error bars depict SEM. Data are the product of two independent repeats. Statistics: an unpaired Student's t test was utilized for comparison in (A), (B), and (H), a one-way ANOVA with a Tukey post hoc test was used in (D), (G), (I), and (J) and with a Bonferroni post hoc in (C).

we did not observe significant antigen-specific IgE in the B1-only mice that were immunized with OVA (Figure 3E). Variable region mapping is an important next step in determination of the IgE-switched B1-clones that are expanded in response to *N. brasiliensis* infection. This will help determine whether there is a preference for enhancement of a particular B1 variable region in this infection.

Pochanke et al. (2007) has described a clone of IgE that is present on FcεRI and can degranulate MCs as early as day 7. This early IgE clone is specific for a pharynx-derived epitope on *N. brasiliensis*, and it does not undergo any somatic hypermuta-tion (SHM) (Pochanke et al., 2007), which is not surprising as germinal centers are minimally developed. The result that specific IgE is made against the parasite is not unexpected, and we would anticipate that this clone would induce MC activation, as exemplified by the PCA (Pochanke et al., 2007). However, there is no evidence that this IgE enhances rejection of the parasite, as we demonstrate with our B2 cells in the RAG1$^{-/-}$ reconstitution model. Also, in our PCA studies (Figures 3F and 3G), *N. brasiliensis* infection caused an inhibition of the PCA reaction, not its complete elimination. Thus, our results are quite compatible with the Pochanke et al. (2007) findings.

The alarmin IL-25 has been shown to be an important regulator of ILC2s. These cells secrete IL-5 after IL-25 stimulation; both cytokines are important for B1 cell IgE production (Figures 4A and 5). Although we know from our depletion studies that T cells are important in the B1 cell IgE response to *N. brasiliensis in vivo*, there is a small basal amount of IgE that remains despite this depletion (Figure 1C). This residual B1 cell IgE may be stimulated by these cytokines directly. The role of T cells and location of interaction with B1 cells warrants further investigation, as mice with B1 cells only do not exhibit germinal centers (data not shown). The cytokine order and amount may be important for IL-5 to further increase IgE production in conjunction with IL-25.

Our studies demonstrate a role for IL-25 in the B1 cell IgE response during helminth infection. Along with other signals, such as IL-4, IL-5, and CD40L stimulation from T cells, IL-25 causes B1 cells to proliferate and enhances CSR to IgE. This IgE binds to MC FcεRI and competes with the binding of parasite-specific IgE that is produced by B2 cells. Traditionally, IgE antibody was not thought to be critical in the clearance of helminth infections since clearance of *N. brasiliensis* was not delayed in IgE$^{-/-}$ mice (Watanabe et al., 1988). In addition, MC-deficient mouse models only exhibit a small delay in *N. brasiliensis* clearance; thus, the role of MCs in this model has also been minimized (Mitchell et al., 1983). The importance of ILC2s (Neill et al., 2010), alternatively activated macrophages (AAMs) (Oeser et al., 2015), and basophils (Liu et al., 2010) in *N. brasiliensis* clearance has certainly been recognized. However, our RAG1$^{-/-}$ reconstitution model demonstrates that IgE activation of MCs can play a host-protective role in *N. brasiliensis* infection. This role is diminished by the B1 cell-produced non-specific IgE. MC degranulation is then no longer evident (Figures 6 and 7; Table S1). Figures 7G and 7H ensure that ILC2 loss was not the cause of the results seen with the anti-ckit antibody; this is in agreement with a recent separate study (Shimokawa et al., 2017). Shimokawa et al. (2017) noted with the use of the anti-ckit antibody, the loss of MCs in the intestines caused a very small reduction in ILC2 number only in the intestinal site due to MC-derived IL-33 that is lost when MCs are deleted. Questions still need to be answered about the effects of anti-ckit treatment on the interstitial cells of Cajal. These cells play a role in intestinal wave activity and are ckit$^+$ (Ordög et al., 1999). The loss of these cells may alter helminth clearance, yet studies utilizing ACK.2 show that the loss of wave activity that leads to muscle quiescence takes 3–4 weeks of treatment (Ordög et al., 1999). Our short anti-ckit treatment regime (Figure 7D) and anti-IgE treatment (Figures 7I and 7J) combine to confirm that IgE binding to the FcεRI is crucial for the B2-mediated enhanced worm expulsion. The lower level of suppression seen with anti-IgE is simply due to a higher *N. brasiliensis* L3 injection in this experiment series; 750 versus 650 L3. While our data do not directly exclude a contribution by IgE binding to the FcεRI on basophils, we note that there were no significant changes in *Mcpt8*, the basophil-specific protease expression (Table S1) (Ugajin et al., 2009). Extrapolating from both Hepworth et al. (2012) and Shimokawa et al. (2017), who have recently highlighted the importance of mast cells in clearance of *H. polygyrus bakeri*, our data support MCs as the primary driver

of this phenotype. Although the RAG1$^{-/-}$ reconstitution model has limitations due to lymphopenia (Figures S5A–S5F), there are clearly sufficient cells to give a strong IgE (Figure 6C) and equivalent IgG1 responses (Figure S5J) as well as mediate the observed clearance (Figures 6A and 6B).

IgE has been long known to be induced during helminth infection, and its role in immunity to parasites is often debated (MacDonald et al., 2002). We hypothesize that in the long evolutionary interaction between helminths and mammals, helminths have developed a mechanism of inducing large amounts of B1 cell IgE that may provide it an evolutionary survival advantage. Slower parasite clearance and increased fecundity leads to increased egg output for the parasite and improved evolutionary success (Quinnell et al., 2004). In summary, this study provides evidence for two opposing roles of IgE in helminth infection. The induction of B1 IgE represents a regulatory mechanism that inhibits MC function and in its absence reveals a previously sidelined role for B2 cell IgE and IgE-mediated MC degranulation in the enhancement of helminth clearance.

EXPERIMENTAL PROCEDURES

Further details and an outline of resources used in this work can be found in Supplemental Experimental Procedures.

Statistical Methods

Error bars represent the standard error of the mean (SEM). A horizontal line with a symbol representing the p value indicates statistical comparison. For pairwise comparisons, Mann-Whitney tests were performed for non-normally distributed data, and Student's t tests were performed for normally distributed data. For multiple comparisons, Kruskal-Wallis tests with Dunn's post hoc were performed for non-normally distributed data, and one-way ANOVA tests with Tukey post hoc or Bonferroni post hoc were performed for normally distributed data. All tests are detailed in the figure legends. A p value of <0.05 was considered significant. All statistical analysis was performed with GraphPad Prism 6 (SCR_002798).

Mice

Mice were kept at Virginia Commonwealth University (VCU) in a barrier vivarium facility in accordance with the humane treatment of laboratory animals sets forth by the National Institutes of Health and the American Association for the Accreditation of Laboratory Animal Care. All mouse protocols were conducted with the permission and oversight of the VCU Institutional Animal Care and Use Committee.

Immunization Models

ACA (Evans et al., 2014) and PCA (Starkl et al., 2016) models were performed as described with the following modifications: i.d. spotting (ACA with OVA-albumin [Sigma-Aldrich] or in PCA with IgE anti-DNP) (Keegan et al., 1991) was done on the pre-shaven flank. Evan's Blue dye (Sigma-Aldrich) was intravenously (i.v.) injected (in ACA immediately following i.d. spot or in PCA 24 hr following mixed with DNP-BSA [Sigma-Aldrich]). Spot size was measured on the back, and back skin was collected for formamide (Sigma-Aldrich) extraction (Evans et al., 2014). For NP Immunizations, NP$_{32}$KLH (LCG BioSearch Technologies) in alum is injected i.p. in 200 μL saline.

RAG1$^{-/-}$ Reconstitution

All naive RAG1$^{-/-}$ mice were i.v. reconstituted with 5×10^6 CD4$^+$ T cells. CD4$^+$ T cells are isolated by first B220$^+$ depletion, followed by anti-mouse L3T4 magnetic bead selection (Miltenyi Biotec) from the spleens of WT mice. Indicated mice were i.v. reconstituted with 10×10^6 naive B2 cells. B2 cells are isolated by depletion using either anti-mouse CD43 Miltenyi microbeads (Miltenyi Biotec) or biotinylated anti-mouse CD43 (AB_493384) followed by anti-biotin

microbeads (Miltenyi Biotec) from the spleens of WT mice. Indicated mice were i.p. reconstituted with $2–4 \times 10^5$ B1 cells. B1 cells are isolated from the peritoneal and pleural cavities of WT mice (Yenson and Baumgarth, 2014). Briefly, cells were Fc blocked on ice for 10 min (2.4G2) (Unkeless, 1979) followed by the following biotinylated antibodies for 30 min on ice: anti-mouse CD23 (B3B4) (AB_312829), anti- mouse CD49b (DX5) (AB_313035), anti-mouse F4/80 (BM8) (AB_893499), anti-mouse CD90.2 (30-H12) (AB_313175), and anti-mouse GR-1 (RB6-8C5) (AB_313368). After washing, anti-biotin microbeads (Miltenyi Biotec) were added, and magnetic bead depletion was performed for B1 enrichment. Mice were not used in experiments until 1 week post reconstitution.

SUPPLEMENTAL INFORMATION

Supplemental Information includes Supplemental Experimental Procedures, five figures, and two tables and can be found with this article online at https://doi.org/10.1016/j.celrep.2018.01.048.

AUTHOR CONTRIBUTIONS

Conceptualization, R.K.M. and D.H.C.; Methodology, R.K.M., J.C.L., and D.H.C.; Validation, R.K.M. and J.C.L.; Formal Analysis, R.K.M., Y.A.V., E.H.D., and J.C.L.; Investigation, R.K.M., S.R.D., Y.A.V., M.P.Z., B.N.J., E.H.D., J.C.L., A.J.L., M.M.D., and L.M.K.; Resources, J.F.U., F.D.F., and D.H.C.; Writing – Original Draft, R.K.M.; Writing – Resources and Editing, J.F.U., F.D.F., S.R.D., D.H.C., J.C.L., and A.J.L.; Visualization, R.K.M. and Y.A.V.; Supervision, R.K.M.; Project Administration, D.H.C.; Funding Acquisition, D.H.C. and R.K.M.

DECLARATION OF INTERESTS

The authors declare no competing interests.

REFERENCES

Ahmed, A., and Koma, M.K. (2015). Interleukin-33 triggers B1 cell expansion and its release of monocyte/macrophage chemoattractants and growth factors. Scand. J. Immunol. 82, 118–124.

Baniyash, M., Kehry, M., and Eshhar, Z. (1988). Anti-IgE monoclonal antibodies directed at the Fc epsilon receptor binding site. Mol. Immunol. 25, 705–711.

Baumgarth, N., Tung, J.W., and Herzenberg, L.A. (2005). Inherent specificities in natural antibodies: a key to immune defense against pathogen invasion. Springer Semin. Immunopathol. 26, 347–362.

Bazaral, M., Orgel, H.A., and Hamburger, R.N. (1973). The influence of serum IgE levels of selected recipients, including patients with allergy, helminthiasis and tuberculosis, on the apparent P-K titre of a reaginic serum. Clin. Exp. Immunol. 14, 117–125.

Brandt, E.B., Strait, R.T., Hershko, D., Wang, Q., Muntel, E.E., Scribner, T.A., Zimmermann, N., Finkelman, F.D., and Rothenberg, M.E. (2003). Mast cells are required for experimental oral allergen-induced diarrhea. J. Clin. Invest. 112, 1666–1677.

Camberis, M., Le Gros, G., and Urban, J., Jr. (2003). Animal model of Nippostrongylus brasiliensis and Heligmosomoides polygyrus. Curr. Protoc. Immunol. Chapter 19, 12.

de Silva, N.R., Brooker, S., Hotez, P.J., Montresor, A., Engels, D., and Savioli, L. (2003). Soil-transmitted helminth infections: updating the global picture. Trends Parasitol. 19, 547–551.

Erickson, L.D., Foy, T.M., and Waldschmidt, T.J. (2001). Murine B1 B cells require IL-5 for optimal T cell-dependent activation. J. Immunol. 166, 1531–1539.

Evans, H., Killoran, K.E., and Mitre, E. (2014). Measuring local anaphylaxis in mice. J. Vis. Exp. (92), e52005.

Finkelman, F.D., Shea-Donohue, T., Morris, S.C., Gildea, L., Strait, R., Madden, K.B., Schopf, L., and Urban, J.F., Jr. (2004). Interleukin-4- and interleukin-13-mediated host protection against intestinal nematode parasites. Immunol. Rev. 201, 139–155.

Fort, M.M., Cheung, J., Yen, D., Li, J., Zurawski, S.M., Lo, S., Menon, S., Clifford, T., Hunte, B., Lesley, R., et al. (2001). IL-25 induces IL-4, IL-5, and IL-13 and Th2-associated pathologies in vivo. Immunity 15, 985–995.

Gerbe, F., Sidot, E., Smyth, D.J., Ohmoto, M., Matsumoto, I., Dardalhon, V., Cesses, P., Garnier, L., Pouzolles, M., Brulin, B., et al. (2016). Intestinal epithelial tuft cells initiate type 2 mucosal immunity to helminth parasites. Nature 529, 226–230.

Gibb, D.R., Saleem, S.J., Kang, D.-J., Subler, M.A., and Conrad, D.H. (2011). ADAM10 overexpression shifts lympho- and myelopoiesis by dysregulating site 2/site 3 cleavage products of Notch. J. Immunol. 186, 4244–4252.

Gurish, M.F., Bryce, P.J., Tao, H., Kisselgof, A.B., Thornton, E.M., Miller, H.R., Friend, D.S., and Oettgen, H.C. (2004). IgE enhances parasite clearance and regulates mast cell responses in mice infected with Trichinella spiralis. J. Immunol. 172, 1139–1145.

Hepworth, M.R., Maurer, M., and Hartmann, S. (2012). Regulation of type 2 immunity to helminths by mast cells. Gut Microbes 3, 476–481.

Hewitson, J.P., Filbey, K.J., Grainger, J.R., Dowle, A.A., Pearson, M., Murray, J., Harcus, Y., and Maizels, R.M. (2011). Heligmosomoides polygyrus elicits a dominant nonprotective antibody response directed against restricted glycan and peptide epitopes. J. Immunol. 187, 4764–4777.

Joseph, M., Auriault, C., Capron, A., Vorng, H., and Viens, P. (1983). A new function for platelets: IgE-dependent killing of schistosomes. Nature 303, 810–812.

Keegan, A.D., Fratazzi, C., Shopes, B., Baird, B., and Conrad, D.H. (1991). Characterization of new rat anti-mouse IgE monoclonals and their use along with chimeric IgE to further define the site that interacts with Fc epsilon RII and Fc epsilon RI. Mol. Immunol. 28, 1149–1154.

Komai-Koma, M., Gilchrist, D.S., McKenzie, A.N.J., Goodyear, C.S., Xu, D., and Liew, F.Y. (2011). IL-33 activates B1 cells and exacerbates contact sensitivity. J. Immunol. 186, 2584–2591.

Kreslavsky, T., Vilagos, B., Tagoh, H., Poliakova, D.K., Schwickert, T.A., Wöhner, M., Jaritz, M., Weiss, S., Taneja, R., Rossner, M.J., and Busslinger, M. (2017). Essential role for the transcription factor Bhlhe41 in regulating the development, self-renewal and BCR repertoire of B-1a cells. Nat. Immunol. 18, 442–455.

Liu, Q., Kreider, T., Bowdridge, S., Liu, Z., Song, Y., Gaydo, A.G., Urban, J.F., Jr., and Gause, W.C. (2010). B cells have distinct roles in host protection against different nematode parasites. J. Immunol. 184, 5213–5223.

MacDonald, A.S., Araujo, M.I., and Pearce, E.J. (2002). Immunology of parasitic helminth infections. Infect. Immun. 70, 427–433.

Madden, K.B., Whitman, L., Sullivan, C., Gause, W.C., Urban, J.F., Jr., Katona, I.M., Finkelman, F.D., and Shea-Donohue, T. (2002). Role of STAT6 and mast cells in IL-4- and IL-13-induced alterations in murine intestinal epithelial cell function. J. Immunol. 169, 4417–4422.

Mitchell, L.A., Wescott, R.B., and Perryman, L.E. (1983). Kinetics of expulsion of the nematode, Nippostrongylus brasiliensis, in mast-cell deficient W/WV mice. Parasite Immunol. *5*, 1–12.

Neill, D.R., Wong, S.H., Bellosi, A., Flynn, R.J., Daly, M., Langford, T.K.A., Bucks, C., Kane, C.M., Fallon, P.G., Pannell, R., et al. (2010). Nuocytes represent a new innate effector leukocyte that mediates type-2 immunity. Nature *464*, 1367–1370.

Oeser, K., Schwartz, C., and Voehringer, D. (2015). Conditional IL-4/IL-13-deficient mice reveal a critical role of innate immune cells for protective immunity against gastrointestinal helminths. Mucosal Immunol. *8*, 672–682.

Oettgen, H.C. (2016). Fifty years later: emerging functions of IgE antibodies in host defense, immune regulation, and allergic diseases. J. Allergy Clin. Immunol. *137*, 1631–1645.

Ordög, T., Ward, S.M., and Sanders, K.M. (1999). Interstitial cells of cajal generate electrical slow waves in the murine stomach. J. Physiol. *518*, 257–269.

Paciorkowski, N., Porte, P., Shultz, L.D., and Rajan, T.V. (2000). B1 B lymphocytes play a critical role in host protection against lymphatic filarial parasites. J. Exp. Med. *191*, 731–736.

Patel, P.S., and Kearney, J.F. (2015). Neonatal exposure to pneumococcal phosphorylcholine modulates the development of house dust mite allergy during adult life. J. Immunol. *194*, 5838–5850.

Perona-Wright, G., Mohrs, K., Taylor, J., Zaph, C., Artis, D., Pearce, E.J., and Mohrs, M. (2008). Cutting edge: helminth infection induces IgE in the absence of mu- or delta-chain expression. J. Immunol. *181*, 6697–6701.

Péry, P., Luffau, G., Charley, J., Petit, A., Rouze, P., and Bernard, S. (1979). Phosphorylcholine antigens from Nippostrongylus brasiliensis. II.–Isolation and partial characterization of phosphorylcholine antigens from adult worm. Ann. Immunol. (Paris) *130*, 889–900.

Pochanke, V., Koller, S., Dayer, R., Hatak, S., Ludewig, B., Zinkernagel, R.M., Hengartner, H., and McCoy, K.D. (2007). Identification and characterization of a novel antigen from the nematode Nippostrongylus brasiliensis recognized by specific IgE. Eur. J. Immunol. *37*, 1275–1284.

Quinnell, R.J., Bethony, J., and Pritchard, D.I. (2004). The immunoepidemiology of human hookworm infection. Parasite Immunol. *26*, 443–454.

Saleem, S.J., Martin, R.K., Morales, J.K., Sturgill, J.L., Gibb, D.R., Graham, L., Bear, H.D., Manjili, M.H., Ryan, J.J., and Conrad, D.H. (2012). Cutting edge: mast cells critically augment myeloid-derived suppressor cell activity. J. Immunol. *189*, 511–515.

Savage, H.P., and Baumgarth, N. (2015). Characteristics of natural antibody-secreting cells. Ann. N Y Acad. Sci. *1362*, 132–142.

Shimokawa, C., Kanaya, T., Hachisuka, M., Ishiwata, K., Hisaeda, H., Kurashima, Y., Kiyono, H., Yoshimoto, T., Kaisho, T., and Ohno, H. (2017). Mast cells are crucial for induction of group 2 innate lymphoid cells and clearance of helminth infections. Immunity *46*, 863–874.e4.

Sinha, P., Clements, V.K., Bunt, S.K., Albelda, S.M., and Ostrand-Rosenberg, S. (2007). Cross-talk between myeloid-derived suppressor cells and macrophages subverts tumor immunity toward a type 2 response. J. Immunol. *179*, 977–983.

Smith, K.G., Light, A., Nossal, G.J., and Tarlinton, D.M. (1997). The extent of affinity maturation differs between the memory and antibody-forming cell compartments in the primary immune response. EMBO J. *16*, 2996–3006.

Starkl, P., Marichal, T., Gaudenzio, N., Reber, L.L., Sibilano, R., Tsai, M., and Galli, S.J. (2016). IgE antibodies, FcεRIα, and IgE-mediated local anaphylaxis can limit snake venom toxicity. J. Allergy Clin. Immunol. *137*, 246–257.e11.

Strait, R.T., Morris, S.C., and Finkelman, F.D. (2006). IgG-blocking antibodies inhibit IgE-mediated anaphylaxis in vivo through both antigen interception and Fc gamma RIIb cross-linking. J. Clin. Invest. *116*, 833–841.

Takatsu, K. (2011). Interleukin-5 and IL-5 receptor in health and diseases. Proc. Jpn. Acad., Ser. B, Phys. Biol. Sci. *87*, 463–485.

Takatsu, K., Takaki, S., Hitoshi, Y., Mita, S., Katoh, S., Yamaguchi, N., and Tominaga, A. (1992). Cytokine receptors on Ly-1 B cells. IL-5 and its receptor system. Ann. N Y Acad. Sci. *651*, 241–258.

Ugajin, T., Kojima, T., Mukai, K., Obata, K., Kawano, Y., Minegishi, Y., Eishi, Y., Yokozeki, H., and Karasuyama, H. (2009). Basophils preferentially express mouse Mast Cell Protease 11 among the mast cell tryptase family in contrast to mast cells. J. Leukoc. Biol. *86*, 1417–1425.

Unkeless, J.C. (1979). Characterization of a monoclonal antibody directed against mouse macrophage and lymphocyte Fc receptors. J. Exp. Med. *150*, 580–596.

Vink, A., Warnier, G., Brombacher, F., and Renauld, J.C. (1999). Interleukin 9-induced in vivo expansion of the B-1 lymphocyte population. J. Exp. Med. *189*, 1413–1423.

von Moltke, J., Ji, M., Liang, H.-E., and Locksley, R.M. (2016). Tuft-cell-derived IL-25 regulates an intestinal ILC2-epithelial response circuit. Nature *529*, 221–225.

Waffarn, E.E., Hastey, C.J., Dixit, N., Soo Choi, Y., Cherry, S., Kalinke, U., Simon, S.I., and Baumgarth, N. (2015). Infection-induced type I interferons activate CD11b on B-1 cells for subsequent lymph node accumulation. Nat. Commun. *6*, 8991.

Watanabe, N., Katakura, K., Kobayashi, A., Okumura, K., and Ovary, Z. (1988). Protective immunity and eosinophilia in IgE-deficient SJA/9 mice infected with Nippostrongylus brasiliensis and Trichinella spiralis. Proc. Natl. Acad. Sci. USA *85*, 4460–4462.

Wu, L.C., and Zarrin, A.A. (2014). The production and regulation of IgE by the immune system. Nat. Rev. Immunol. *14*, 247–259.

Yenson, V., and Baumgarth, N. (2014). Purification and immune phenotyping of B-1 cells from body cavities of mice. Methods Mol. Biol. *1190*, 17–34.

Supplemental Information

B1 Cell IgE Impedes Mast Cell-Mediated Enhancement

of Parasite Expulsion through B2 IgE Blockade

Rebecca K. Martin, Sheela R. Damle, Yolander A. Valentine, Matthew P. Zellner, Briana N. James, Joseph C. Lownik, Andrea J. Luker, Elijah H. Davis, Martha M. DeMeules, Laura M. Khandjian, Fred D. Finkelman, Joseph F. Urban Jr., and Daniel H. Conrad

Supplemental Information

B1 Cell IgE Impedes Mast Cell-Mediated Enhancement

of Parasite Expulsion through B2 IgE Blockade

Rebecca K. Martin, Sheela R. Damle, Yolander A. Valentine, Matthew P. Zellner, Briana N. James, Joseph C. Lownik, Andrea J. Luker, Elijah H. Davis, Martha M. DeMeules, Laura M. Khandjian, Fred D. Finkelman, Joseph F. Urban Jr., and Daniel H. Conrad

Supplemental Experimental Procedures

CONTACT FOR REAGENT AND RESOURCE SHARING

Further information and requests for resources and reagents should be directed to and will be fulfilled by the Lead Contact, Daniel Conrad (Daniel.Conrad@vcuhealth.org).

EXPERIMENTAL MODEL AND SUBJECT DETAIL

Mice
Mice were kept at Virginia Commonwealth University (VCU) in a barrier vivarium facility in accordance with the humane treatment of laboratory animals sets forth by the National Institutes of Health and the American Association for the Accreditation of Laboratory Animal Care. All mouse protocols were conducted with the permission and oversight of the VCU Institutional Animal Care and Use Committee. Sex was randomized between groups, including both males and females. Differences between sexes were not observed (data not shown). Mice ages ranged between 6 and 16 weeks for all experiments with an approximate body weight of 20 grams. ADAM10Tg mice were generated as described in *Gibb et al.* and have been continuously backcrossed an additional 20 generations to the C57BL6/J background (Gibb *et al.*, 2011). Littermates were used as WT controls. RAG1$^{-/-}$ mice (IMSR_JAX:002216) and BALB/c RAG1$^{-/-}$ mice (IMSR_JAX:003145) were purchased from The Jackson Laboratory and maintained through breeding. WT (IMSR_JAX:000664) and BALB/c WT (IMSR_JAX:000651) mice were also purchased from The Jackson Laboratory and maintained through breeding. IgE$^{-/-}$ (MGI:3603569) mice were a gift from Hans Oettgen and Mitch Grayson and were generated as described (Oettgen *et al.*, 1994). IL-25R$^{-/-}$ mice (*IL17rb$^{-/-}$*) were a gift from Yui Hsi Wang. They were generated as described(Lee *et al.*, 2016). IL-25R$^{-/-}$, IgE$^{-/-}$, WT, and BALB/c WT mice were used to harvest cells for reconstitution experiments in strain paired RAG1$^{-/-}$ mice. Cells were harvested from both male and female donor mice, mixed and then adoptively transferred into male and female recipient mice.

METHOD DETAILS

Parasite lifecycles, infection, and NES preparation
The life cycles of both *N. brasiliensis* and *H. polygyrus bakeri* were maintained as previously described (Camberis, Le Gros and Urban, 2003). Infective larvae (L3) were prepared from mouse fecal cultures. 650 *N. brasiliensis* L3 (unless otherwise noted) were injected *s.c.* into experimental mice. 200 *H. polygyrus bakeri* L3 were inoculated i.g.. Mice were monitored for eggs per gram of feces (EPG) by collecting feces by weight and resuspending in flotation solution (Saturated NaCl solution) based on 1 gram feces to 60mL of flotation solution, followed by counting two chambers in a McMaster Counting Slide (Chalex, LLC.), taking the average, and multiplying by 400 to obtain EPG (Finkelman *et al.*, 2004; Saleem *et al.*, 2012; Martin *et al.*, 2014). Day 7 intestinal worms were recovered for counting, utilizing the proximal half of the small intestine longitudinally bisected and suspended in 37°C PBS in cheesecloth (Camberis, Le Gros and Urban, 2003). NES extract was generated from adult worms as described(Camberis, Le Gros and Urban, 2003).

GEM, GK1.5, 2.43, ACK.2, and R1E4 treatment
For MDSC depletion, 1.5mg/mouse gemcitabine (GEM) (Eli Lilly and Company) in 200µL saline was injected *i.p.* on day 0 and every 5 days following until the conclusion of the experiment (Saleem *et al.*, 2012). For T cell depletion, 200µg anti-CD4 (GK1.5)(Wilde *et al.*, 1983) and anti-CD8a (2.43)(Sarmiento, Glasebrook and Fitch, 1980) antibodies or 200µg control Rat IgG were injected *i.p.* in 200µL saline on days -3, -2, -1, 0, 5, and 10 (Saleem *et al.*, 2012). For mucosal MC depletion, 1mg of anti-ckit (ACK.2)(Nishikawa *et al.*, 1986) or control Rat IgG was injected in 200µL saline on days 1, 2, 3, 4, 5, and 6. The initial dose was *i.v.*, then subsequent doses were administered *i.p.* as described previously(Brandt *et al.*, 2003). Treatment began 24 hours after *N. brasiliensis* inoculation. For anti-IgE (R1E4) treatment, 100µg was injected daily *i.p.* starting at reconstitution and continuing until experimental completion(Baniyash, Kehry and Eshhar, 1988; Keegan *et al.*, 1991).

Total IgE, IgG1, and IgM ELISA
For total IgE ELISA, briefly, plates were coated with 5µg/mL of rat anti-mouse IgE (B1E3)(Keegan *et al.*, 1991) in borate buffered saline, blocked (PBS with 0.02% Tween20 and 2% FBS), detected with biotin rat anti-mouse IgE (R1E4) and Streptavidin-Alkaline phosphatase (Southern Biotech). Plates were developed with phosphate tablets

(Sigma-Aldrich) dissolved in substrate buffer (0.1g $MgCl_2.6H_2O$, 0.2 NaN_3, 50mL diethanolamine, pH to 9.8 per 500mL). Absorbance was measured at 405nm - 650nm(Damle *et al.*, 2016). IgE standard was purified mouse IgE anti-DNP antibody(Keegan *et al.*, 1991). Fold IgE (Fig 5A) was calculated for each replicate by dividing the condition with IL-25 (for each dose) by the cells sorted from the same mouse without IL-25. For total IgG1 levels, plates were coated with 5µg/mL of goat-anti mouse IgG-UNLB (Southern Biotech) and detected with goat anti-mouse IgG1-AP (Southern Biotech)(Chaimowitz *et al.*, 2011). For total IgM levels, plates were coated with 5µg/mL of goat-anti mouse IgM-UNLB (Southern Biotech) and detected with goat anti-mouse IgM-AP (Southern Biotech). All ELISAs were read using SoftMax Pro Data Acquisition and Analysis Software (Molecular Devices) on a Molecular Devices Plate reader (Molecular Devices).

NP and OVA-specific ELISAs
For NP-specific ELISAs, plates were coated with $NP_{25}BSA$ for total affinity and NP_4BSA for high affinity antibody measurement (LCG BioSearch Technologies) and detected as with total Ig assays (Smith *et al.*, 1997). For OVA-specific IgE ELISAs briefly, plates were coated with 5µg/mL of anti-IgE (R1E4), blocked with SuperBlock Dry Blend Blocking Buffer (Thermo Fisher Scientific), standard was IgE anti-DNP, secondary was OVA-DNP-Biotin, and was streptavidin-AP (Southern Biotech).

Histamine and MCPT-1 ELISAs
For ELISA on mucus, one third of the jejunal tissue harvested, dissected open and mucus was gently scraped from the lumen. The mucus was then weighed and flash frozen in a 1.5mL tube. Immediately prior to performing ELISA, mucus was resuspended in 50µL ELISA dilution buffer per 0.01g wet weight. Histamine (Neogen) and MCPT-1 (AB_2575142) ELISAs were performed as directed by manufacturer.

B cell Culture
Cells were plated in cRPMI 1640 containing 10% FBS, 2mM L-glutamine, 50µM 2-mercaptoethanol, 100 U/mL penicillin, 100g/mL streptomycin, 1mM HEPES (Quality Biological), and 1mM sodium pyruvate (Corning Cellgro) at indicated concentrations. Cytokines (10ng/mL rIL-4 (PeproTech), 2µL/mL anti-CD40 (HM40-3) (AB_312944), 300ng/mL rIL-5 (Peprotech), 50 ng/mL IL-33(Biolegend)(Komai-Koma *et al.*, 2011; Ahmed and Koma, 2015), rIL-25 (Biolegend), various concentrations) were added. Cell-free supernatants were harvested at days 5, 7, or 9, or cells were harvested at day 4 or 5. For *in vivo* experiments with IL-33, rIL-33 was injected *i.p.* daily at 2µg/mouse for 7 days prior to sorting.

Flow Cytometry and Cell Sorting
Peritoneal lavage, MLNs, lungs, and spleens were collected. Lungs were digested with collagenase I (Worthington) prior to obtaining a single cell suspension. MLNs were teased apart and all other organs were ground between two glass slides. Red blood cells were removed by ACK lysis buffer (Sigma-Aldrich) when needed. The cell suspension was flushed through a 40µm mesh cell strainer. After Fc blocking (2.4G2)(Unkeless, 1979), labeled antibodies were added at concentrations recommended by the manufacturer. Flow data was collected with a LSRFortessa or FACSAria II (BD Biosciences), using BDFACSDiva™ 8.0 (BD Biosciences) and analyzed with Flowjo v7.6.5 (BD Biosciences). Anti-mouse antibodies used were Pe-Cy7 or Biotin conjugated anti-CD11b (M1/70)(AB_312798, AB_312787), BV421 conjugated anti-CD23 (B3B4)(AB_2563599), APC, PE, or Biotin conjugated anti-B220 (RA3-6B2)(AB_312996,AB_394620,AB_312989), PE conjugated anti-CD4 (GK1.5)(AB_312692), FITC conjugated anti-Ly6G (1A8)(AB_1236494), APC conjugated anti-Ly6C (HK1.4)(AB_1732076), PE conjugated anti-CD138 (281-2)(AB_10916119), Zombie Aqua Live/Dead Viability Kit, APCFIRE-conjugated anti-CD45 (30-F11)(AB_2572116), BV786 conjugated anti-ICOS (C398.4A)(AB_2629729), BV605 conjugated anti-CD90.2 (Thy1.2)(AB_11203724), and BV421 conjugated anti-Sca1 (D7)(AB_10898327), FITC conjugated anti-CD3ε (500A2) (AB_394620), FITC or Biotin conjugated anti-CD3ε (145-2C11)(AB_312671,AB_312669), Biotin conjugated anti-TER-119 (AB_313704), and Biotin conjugated anti-GR1 (RB6-8C5)(AB_313368). Biotinylated antibodies were followed by Streptavidin-PE(Biolegend). When more than one BV antibody was used, Brilliant Violet Stain Buffer was utilized according to the manufacturer's protocol (BD Biosciences).

qRT-PCR
For Fig 5F, S1C, and S2F, cells were isolated and total RNA was extracted using TRIzol reagent (Thermo Fisher Scientific). RNA was reverse-transcribed using Superscript IV (Thermo Fisher Scientific). Control RNA samples were made without Superscript IV utilizing the same temperature protocol. 20ng of equivalent RNA was used per reaction in duplicate. Primers (Resource Table) were utilized in a Power Up SYBR Green (Thermo Fisher

Scientific) RT-PCR assay or Taqman probes (Resource Table) were utilized with TaqMan™ Universal PCR Master Mix (Thermo Fisher Scientific). For Fig 7C, Table S1 and S2, jejunal and lung RNA was isolated after flash freezing in TRIzol reagent (Thermo Fisher Scientific) followed by mechanical homogenization. 35µg of total RNA was reverse transcribed using oligo-d(T)$_{20}$ primers for only mRNA. cDNA was used at a final dilution of 1:20 per reaction. Each reaction was carried out in duplicate. Primers were designed using NCBI PrimerBlast and were designed to span exon junctions. Specificity was confirmed using NCBI PrimerBlast. Primers used for Table S1 and S2 (Eurofins or Thermo Fisher Scientific) are listed in Supplemental Experimental Procedures Table 1. For Fig 7C, Table S1 and S2 qRT-PCR amplification was conducted with 45 cycles of annealing and elongation at 60°C for 20 seconds with 1 second melting at 95°C. All qRT-PCR was run using QuantStudio 3 real-time PCR system and Thermo Fisher Cloud analysis software (Thermo Fisher Scientific).

Histology
Jejunum tissue was collected 10-12cm distal to the stomach, fixed in ten percent formalin, embedded in paraffin, sectioned, and mounted on slides. Tissue processing from post-fixation to mounting on slides was performed by Histo-Scientific Research Laboratories. 5-µm sections were then de-paraffinized followed by staining for mucosal MCs with chloroacetate (specific esterase) staining as directed (Sigma-Aldrich). Slides were visualized and images were taken on an Olympus BX41 microscope.

RESOURCE TABLE

REAGENT or RESOURCE	SOURCE	IDENTIFIER
Antibodies		
PE/Cy7 Rat Anti-Mouse/Human CD11b antibody(M1/70)(Lot#B227804)	Biolegend	Cat#101216; AB_312798
Biotin Rat Anti-Mouse/Human CD11b antibody(M1/70) (Lot#B221905)	Biolegend	Cat#101204; AB_312787
Brilliant Violet 421 Rat Anti-Mouse CD23 antibody(B3B4) (Lot#B236144)	Biolegend	Cat#101621; AB_2563599
Biotin Rat Anti-Mouse CD23 antibody(B3B4) (Lot#B200229)	Biolegend	Cat#101604; AB_312829
APC Rat Anti-Mouse/Human CD45R/B220 antibody(RA3-6B2) (Lot#B189921, B208579)	Biolegend	Cat#103212; AB_312996
PE Rat Anti-Mouse CD45R/B220 antibody(RA3-6B2) (Lot#74790)	BD Biosciences	Cat#553090; AB_394620
Biotin Rat Anti-Mouse/Human CD45R/B220 antibody(RA3-6B2) (Lot#B226660)	Biolegend	Cat#103204; AB_312989
PE Rat Anti-Mouse CD4 antibody(GK1.5)(Lot#B196677)	Biolegend	Cat#100407; AB_312692
FITC Rat Anti-Mouse Ly-6G antibody(1A8)(Lot#B163428)	Biolegend	Cat#127606; AB_1236494
APC Rat Anti-Mouse Ly-6C antibody(HK1.4) (Lot#B161489)	Biolegend	Cat#128016; AB_1732076
PE Rat Anti-Mouse CD138 (Syndecan-1) antibody(281-2) (Lot#B182508)	Biolegend	Cat#142504; AB_10916119
APC/Fire 750 Rat Anti-Mouse CD45 antibody(30-F11) (Lot#B226658)	Biolegend	Cat#103154; AB_2572116
Brilliant Violet 785 Hamster Anti-Human/Mouse/Rat CD278 (ICOS) antibody(C398.4A)(Lot#B235753)	Biolegend	Cat#313534; AB_2629729
Brilliant Violet 605 Rat Anti-Mouse CD90.2 (Thy1.2) antibody(Lot#B241066)	Biolegend	Cat#140318; AB_11203724
Biotin Rat Anti-Mouse CD90.2 antibody (30-H12)(Lot#B217943, B243047, B241136)	Biolegend	Cat#105304; AB_313175
Brilliant Violet 421 Rat Anti-Mouse Ly-6A/E (Sca-1) antibody(D7)(Lot#B202856)	Biolegend	Cat#108128; AB_10898327

FITC Hamster Anti-Mouse CD3ε antibody(145-2C11)(Lot#B182508)	Biolegend	Cat#100306; AB_312671
Biotin Hamster Anti-Mouse CD3ε antibody(145-2C11)(Lot#B240049, B216147)	Biolegend	Cat#100306; AB_312669
FITC Hamster Anti-Mouse CD3ε antibody(500A2)	Biolegend	Cat#152304; AB_2632667
Biotin Rat Anti-Mouse TER-119/Erythroid Cells antibody(Lot#B247740, B218645)	Biolegend	Cat#116204; AB_313704
Biotin Rat Anti-Mouse Ly-6G/Ly-6C (Gr-1) antibody (RB6-8C5)(Lot#B236916, B200655)	Biolegend	Cat#108404; AB_313368
Biotin Rat Anti-Mouse CD43 Activation-Associated Glycoform antibody (1B11)(Lot#B214275)	Biolegend	Cat#121204; AB_493384
Biotin Rat Anti-Mouse CD49b antibody(DX5)(Lot#B232367, B215293)	Biolegend	Cat#108904; AB_313035
Biotin Rat Anti-Mouse F4/80 antibody(BM8)(Lot#B234292, B206030)	Biolegend	Cat#123106; AB_893499
Purified Hamster Anti-Mouse CD40 antibody(HM40-3)(Lot#B174833)	Biolegend	Cat#102902; AB_312944
Goat Anti-Mouse IgG1, Human Ads-AP(Lot#B8613-VB04E)	Southern Biotech	Cat#1070-04
Goat Anti-Mouse IgM, Human Ads-AP(Lot#D2013-R653C)	Southern Biotech	Cat#1020-04
Goat Anti-Mouse IgG, Human Ads-UNLB(Lot#K3515-X447)	Southern Biotech	Cat#1030-01
Goat Anti-Mouse IgM, Human Ads-UNLB(Lot#K2915-QF36)	Southern Biotech	Cat#1020-01
CD4 (L3T4) MicroBeads, mouse(Lot#5170526210)	Miltenyi Biotec	Cat#130-117-043
CD43 (Ly-48) MicroBeads, mouse	Miltenyi Biotec	Cat#130-049-801
Anti-Biotin MicroBeads(Lot#5170630319)	Miltenyi Biotec	Cat#130-090-485
Purified Rat Anti-Mouse IgE (B1E3) antibody	Isolated from hybridoma(Keegan *et al.*, 1991)	N/A
Biotin-Purified Rat Anti-Mouse IgE (R1E4) antibody	Isolated from hybridoma(Keegan *et al.*, 1991)	N/A
Purified Rat Anti-Mouse CD16 / CD32 (2.4G2) antibody	Isolated from hybridoma(Unkeless, 1979)	N/A
Purified Rat Anti-Mouse ckit (ACK.2) antibody	Laboratory of Fred Finkelman(Nishikawa *et al.*, 1986)	N/A
Purified Rat Anti-Mouse CD8a (2.43) antibody	Isolated from hybridoma(Sarmiento, Glasebrook and Fitch, 1980)	N/A
Purified Rat Anti-Mouse CD4 (GK1.5) antibody	Isolated from hybridoma(Wilde *et al.*, 1983)	N/A
Purified Mouse IgE anti-DNP antibody	Isolated from hybridoma(Keegan *et al.*, 1991)	N/A
Chemicals, Peptides, and Recombinant Proteins		
Streptavidin-Phycoerythrin, SAv-PE(Lot#B243518)	Biolegend	Cat#405204
Zombie Aqua™ Fixable Viability Kit(Lot#B241805)	Biolegend	Cat#423102

Brilliant Stain Buffer	BD Biosciences	Cat#566349
Streptavidin-AP(Lot#H0016-v566E)	Southern Biotech	Cat#7100-04
Recombinant Murine IL-4 (Lot#111249)	Peprotech	Cat#214-14
Recombinant Murine IL-5 (Lot#1206406)	Peprotech	Cat#215-15
Recombinant Murine IL-33 (Lot#B223367)	Biolegend	Cat#580506
Recombinant Murine IL-25(IL-17E)(Insect expressed, CF)(Lot#B213181, B213180, B173762)	Biolegend	Cat#587306
NP-KLH (Keyhole Limpet Hemocyanin)	LGC BioSearch Technologies	Cat#N-5060-25
NP-BSA (Bovine Serum Albumin), Ratio > 20	LGC BioSearch Technologies	Cat#N-5050H-100
NP-BSA (Bovine Serum Albumin), Ratio 1-4	LGC BioSearch Technologies	Cat#N-5050XL-100
SuperBlock™ (TBS) Blocking Buffer Dry Blend	Thermo Fisher Scientific	Cat#37545
OVA-DNP-Biotin	This paper(Damle *et al.*, 2018)	N/A
SuperScript™ IV Reverse Transcriptase	Thermo Fisher Scientific	Cat#18090010
PowerUp™ SYBR™ Green Master Mix	Thermo Fisher Scientific	Cat#A25742
Gemzar® (Gemcitabine)	Eli Lilly and Company	NDC Code#0002-7501-01
DNP-BSA (Albumin from Bovine Serum (BSA), 2,4-Dinitrophenylated)	Thermo Fisher Scientific	Cat#A23018
N. brasiliensis Excretory Secretory Extract	This paper(Camberis, Le Gros and Urban, 2003)	N/A
Albumin from chicken egg white (OVA)	Sigma-Aldrich	Cat#A5503; CAS: 9006-59-1
Formamide	Sigma-Aldrich	Cat#F9037; CAS: 75-12-7
Evan's blue	Sigma-Aldrich	Cat#E2129; CAS: 314-13-6
Collagenase I (Lot#44K15158A)	Worthington	Cat#LS004196; CAS: 9001-12-1
TaqMan™ Universal PCR Master Mix	Thermo Fisher Scientific	Cat#4304437
Critical Commercial Assays		
Histamine Kit, 96 well kit(Lot#245546)	Neogen	Cat#409010
Mouse MCPT-1 (mMCP-1) ELISA Ready-SET-Go!¨ 10 x 96 tests w/plates Kit antibody	Thermo Fisher Scientific	Cat#88-7503-86; AB_2575142
Deposited Data		
Gene Expression Analysis in Jejunum and Lung	This Paper	Table S1, Table S2
Experimental Models: Organisms/Strains		
Mouse: RAG1$^{-/-}$: B6.129S7-*Rag1^{tm1Mom}/J*	The Jackson Laboratory	IMSR_JAX:002216
Mouse: WT: C57BL/6J	The Jackson Laboratory	IMSR_JAX:000664
Mouse: BALB/c RAG1$^{-/-}$: C.129S7(B6)-Rag1^{tm1Mom}/J	The Jackson Laboratory	IMSR_JAX:003145
Mouse: BALB/c WT: BALB/cJ	The Jackson Laboratory	IMSR_JAX:000651

Mouse: IgE^{-/-}: Igh-7[tm1Led]/Igh-7[tm1Led]	Hans Oettgen(Oettgen *et al.*, 1994)	MGI:3603569
Mouse: IL-25R^{-/-}: IL17rb^{-/-}	Yui-His Wang(Lee *et al.*, 2016)	N/A
Mouse: ADAM10Tg: Tg(ADAM10)2Dhc	Daniel Conrad(Gibb *et al.*, 2011)	N/A
N. brasiliensis	Joseph Urban, Jr.(Camberis, Le Gros and Urban, 2003)	N/A
H. polygyrus bakeri	Joseph Urban, Jr.(Camberis, Le Gros and Urban, 2003)	N/A
Oligonucleotides		
Secreted *Ighe* 5'-GTCGCCTAGAGGTCGCCAAG-3'	Integrated DNA Technologies(He *et al.*, 2013)	N/A
Secreted *Ighe* 5'-CATCCACCTTCCCCACCACAGC-3'	Integrated DNA Technologies(He *et al.*, 2013)	N/A
Secreted *Ighg1* 5'-TGCACAACCACCATACTGAGA-3'	Integrated DNATechnologies(He *et al.*, 2013)	N/A
Secreted *Ighg1* 5'-GGGTGGAGGTAGGTGTCAGA-3'	Integrated DNA Technologies(He *et al.*, 2013)	N/A
Actb 5'-CAATAGTGATGACCTGGCCGT-3'	Integrated DNA Technologies(Weber *et al.*, 2015)	N/A
Actb 5'-AGAGGGAAATCGTGCGTGAC-3'	Integrated DNA Technologies(Weber *et al.*, 2015)	N/A
Mouse *Adam10* (Mm00545742_m1)	Thermo Fisher Scientific	Cat#4331182
Mouse *Gapdh* (Mm99999915_g1)	Thermo Fisher Scientific	Cat#4331182
See Supplemental Experimental Procedures Table 1 for a full list of primers	This Paper	N/A
Software and Algorithms		
Graphpad Prism 6	GraphPad	SCR_002798; https://www.graphpad.com
SoftMax Pro Data Acquisition and Analysis Software	Molecular Devices	SCR_014240; https://www.moleculardevices.com
FlowJo 7.6.5	BD Biosciences	https://www.flowjo.com/solutions/flowjo/downloads
BDFACSDiva™ 8.0	BD Biosciences	http://www.bdbiosciences.com/us/instruments/research/software/flow-cytometry-acquisition/bd-facsdiva-software/m/111112/overview

Thermo Fisher Cloud	Thermo Fisher Scientific	https://www.thermofisher.com/us/en/home/cloud.html
Other		
Two-Chamber Opaque McMaster Slide	Chalex, LLC	Cat#2CO

REFERENCES

Ahmed, A. and Koma, M. K. (2015) 'Interleukin-33 Triggers B1 Cell Expansion and Its Release of Monocyte/Macrophage Chemoattractants and Growth Factors.', *Scandinavian journal of immunology*, 82(2), pp. 118–24. doi: 10.1111/sji.12312.

Baniyash, M., Kehry, M. and Eshhar, Z. (1988) 'Anti-IgE monoclonal antibodies directed at the Fc epsilon receptor binding site.', *Molecular immunology*, 25(8), pp. 705–11. Available at: http://www.ncbi.nlm.nih.gov/pubmed/2460756.

Brandt, E. B., Strait, R. T., Hershko, D., Wang, Q., Muntel, E. E., Scribner, T. A., Zimmermann, N., Finkelman, F. D. and Rothenberg, M. E. (2003) 'Mast cells are required for experimental oral allergen-induced diarrhea.', *The Journal of clinical investigation*. American Society for Clinical Investigation, 112(11), pp. 1666–77. doi: 10.1172/JCI19785.

Camberis, M., Le Gros, G. and Urban, J. (2003) 'Animal model of Nippostrongylus brasiliensis and Heligmosomoides polygyrus.', *Current protocols in immunology / edited by John E. Coligan ... [et al.]*, Chapter 19, p. Unit 19.12. doi: 10.1002/0471142735.im1912s55.

Chaimowitz, N. S., Martin, R. K., Cichy, J., Gibb, D. R., Patil, P., Kang, D.-J., Farnsworth, J., Butcher, E. C., McCright, B. and Conrad, D. H. (2011) 'A disintegrin and metalloproteinase 10 regulates antibody production and maintenance of lymphoid architecture.', *Journal of immunology (Baltimore, Md. : 1950)*, 187(10), pp. 5114–22. doi: 10.4049/jimmunol.1102172.

Damle, S. R., Martin, R. K., Cockburn, C. L., Lownik, J. C., Carlyon, J. A., Smith, A. D. and Conrad, D. H. (2018) 'ADAM10 and Notch1 on murine dendritic cells control the development of type 2 immunity and IgE production', *Allergy*, 73(1), pp. 125–136. doi: 10.1111/all.13261.

Damle, S. R., Martin, R. K., Cross, J. V and Conrad, D. H. (2016) 'Macrophage migration inhibitory factor deficiency enhances immune response to Nippostrongylus brasiliensis.', *Mucosal immunology*. doi: 10.1038/mi.2016.29.

Finkelman, F. D., Shea-Donohue, T., Morris, S. C., Gildea, L., Strait, R., Madden, K. B., Schopf, L. and Urban, J. F. (2004) 'Interleukin-4- and interleukin-13-mediated host protection against intestinal nematode parasites.', *Immunological reviews*, 201, pp. 139–55. doi: 10.1111/j.0105-2896.2004.00192.x.

Gibb, D. R., Saleem, S. J., Kang, D.-J., Subler, M. A. and Conrad, D. H. (2011) 'ADAM10 overexpression shifts lympho- and myelopoiesis by dysregulating site 2/site 3 cleavage products of Notch.', *Journal of immunology (Baltimore, Md. : 1950)*, 186(7), pp. 4244–52. doi: 10.4049/jimmunol.1003318.

He, J.-S., Meyer-Hermann, M., Xiangying, D., Zuan, L. Y., Jones, L. A., Ramakrishna, L., de Vries, V. C., Dolpady, J., Aina, H., Joseph, S., Narayanan, S., Subramaniam, S., Puthia, M., Wong, G., Xiong, H., Poidinger, M., Urban, J. F., Lafaille, J. J. and Curotto de Lafaille, M. A. (2013) 'The distinctive germinal center phase of IgE+ B lymphocytes limits their contribution to the classical memory response.', *The Journal of experimental medicine*. The Rockefeller University Press, 210(12), pp. 2755–71. doi: 10.1084/jem.20131539.

Keegan, A. D., Fratazzi, C., Shopes, B., Baird, B. and Conrad, D. H. (1991) 'Characterization of new rat anti-mouse IgE monoclonals and their use along with chimeric IgE to further define the site that interacts with FcεRII and FcεRI', *Molecular Immunology*, 28(10), pp. 1149–1154. doi: 10.1016/0161-5890(91)90030-N.

Komai-Koma, M., Gilchrist, D. S., McKenzie, A. N. J., Goodyear, C. S., Xu, D. and Liew, F. Y. (2011) 'IL-33 activates B1 cells and exacerbates contact sensitivity.', *Journal of immunology (Baltimore, Md. : 1950)*, 186(4), pp. 2584–91. doi: 10.4049/jimmunol.1002103.

Lee, J.-B., Chen, C.-Y., Liu, B., Mugge, L., Angkasekwinai, P., Facchinetti, V., Dong, C., Liu, Y.-J., Rothenberg, M. E., Hogan, S. P., Finkelman, F. D. and Wang, Y.-H. (2016) 'IL-25 and CD4+ TH2 cells enhance type 2 innate lymphoid cell–derived IL-13 production, which promotes IgE-mediated experimental food allergy', *Journal of Allergy and Clinical Immunology*, 137(4), p. 1216–1225.e5. doi: 10.1016/j.jaci.2015.09.019.

Martin, R. K., Saleem, S. J., Folgosa, L., Zellner, H. B., Damle, S. R., Nguyen, G.-K. T., Ryan, J. J., Bear, H. D., Irani, A.-M. and Conrad, D. H. (2014) 'Mast cell histamine promotes the immunoregulatory activity of myeloid-derived suppressor cells.', *Journal of leukocyte biology*. doi: 10.1189/jlb.5A1213-644R.

Nishikawa, S. I., Sasaki, Y., Kina, T., Amagai, T. and Katsura, Y. (1986) 'A monoclonal antibody against Igh6-4 determinant', *Immunogenetics*. Springer-Verlag, 23(2), pp. 137–139. doi: 10.1007/BF00377976.

Oettgen, H. C., Martin, T. R., Wynshaw-Boris, A., Deng, C., Drazen, J. M. and Leder, P. (1994) 'Active anaphylaxis in IgE-deficient mice.', *Nature*, 370(6488), pp. 367–70. doi: 10.1038/370367a0.

Saleem, S. J., Martin, R. K., Morales, J. K., Sturgill, J. L., Gibb, D. R., Graham, L., Bear, H. D., Manjili, M. H., Ryan, J. J. and Conrad, D. H. (2012) 'Cutting edge: mast cells critically augment myeloid-derived suppressor cell activity.', *Journal of immunology (Baltimore, Md. : 1950)*, 189(2), pp. 511–5. doi: 10.4049/jimmunol.1200647.

Sarmiento, M., Glasebrook, A. L. and Fitch, F. W. (1980) 'IgG or IgM monoclonal antibodies reactive with different determinants on the molecular complex bearing Lyt 2 antigen block T cell-mediated cytolysis in the absence of complement.', *Journal of immunology (Baltimore, Md. : 1950)*, 125(6), pp. 2665–2672. Available at: http://www.ncbi.nlm.nih.gov/pubmed/6159417.

Smith, K. G., Light, A., Nossal, G. J. and Tarlinton, D. M. (1997) 'The extent of affinity maturation differs between the memory and antibody-forming cell compartments in the primary immune response.', *The EMBO journal*, 16(11), pp. 2996–3006. doi: 10.1093/emboj/16.11.2996.

Unkeless, J. C. (1979) 'Characterization of a monoclonal antibody directed against mouse macrophage and lymphocyte Fc receptors.', *Journal of Experimental Medicine*. Rockefeller University Press, 150(3), pp. 580–596. doi: 10.1084/jem.150.3.580.

Weber, C. E., Kothari, A. N., Wai, P. Y., Li, N. Y., Driver, J., Zapf, M. A. C., Franzen, C. A., Gupta, G. N., Osipo, C., Zlobin, A., Syn, W. K., Zhang, J., Kuo, P. C. and Mi, Z. (2015) 'Osteopontin mediates an MZF1-TGF-β1-dependent transformation of mesenchymal stem cells into cancer-associated fibroblasts in breast cancer', *Oncogene*. Nature Publishing Group, 34(37), pp. 4821–4833. doi: 10.1038/onc.2014.410.

Wilde, D. B., Marrack, P., Kappler, J., Dialynas, D. P. and Fitch, F. W. (1983) 'Evidence implicating L3T4 in class II MHC antigen reactivity; monoclonal antibody GK1.5 (anti-L3T4a) blocks class II MHC antigen-specific proliferation, release of lymphokines, and binding by cloned murine helper T lymphocyte lines.', *Journal of immunology (Baltimore, Md. : 1950)*. American Association of Immunologists, 131(5), pp. 2178–83. Available at: http://www.ncbi.nlm.nih.gov/pubmed/6195255.

	Forward	**Reverse**
Ccl2	GGCTCAGCCAGATGCAGTTA	GAGTAGCAGCAGGTGAGTGG
Chil3	AGGAAGCCCTCCTAAGGACA	CTCCACAGATTCTTCCTCAAAAGC
Cma1	CTGCTCCTTCTCCTGGGTTCC	TGTTATAGACCTTCCCGCACAGT
Cpa3	AACTGCCTCCTAACCACCAG	AGTCTTGTAAATTGTGGATGCTATT
Fcer1a	GCACTGCTGTTCATGTCTCTTG	AATCCATGGTGGGTCCAAGG
Fcgbp	GAAGGGTGTGAGTGCGATGA	GGGAAGAGTTCACCGGCATA
Hprt	CAGGGATTTGAATCACGTTTGTG	TTGCAGATTCAACTTGCGCT
Il13	CACACAAGACCAGACTCCCC	GTTGGTCAGGGAATCCAGGG
Il22	CTCCTGTCACATCAGCGGT	CAGTTCCCCAATCGCCTTGA
Il25	TATGAGTTGGACAGGGACTTGA	TGGTAAAGTGGGACGGAGTTG
Il33	GACCAGGTGCTACTACGCT	CACACCGTCGCCTGATTGAC
Il4	CCATATCCACGGATGCGACA	CTGTGGTGTTCTTCGTTGCTG
Il5	AGCAATGAGACGATGAGGCTT	CCCCCACGGACAGTTTGATT
Il6	CCACTTCACAAGTCGGAGGC	TTGCCATTGCACAACTCTTTTCT
Il9	GCTGCTTGTGTCTCTCCGTC	TGGTTGCATGGCTTTTCGC
Mcpt1	AGCTGGAGCTGAGGAGATTATT	GTCCTCAGAACCTCTGTCCG
Mcpt2	GAAGCTCACCAAGGCCTCAA	CACCAATAATCTCCTCAGCTCCA
Mcpt4	GTGGGCAGTCCCAGAAAGAAA	TCCAGAGTCTCCCTTGTATGCT
Muc1	TACCACACTCACGGACGCTA	CCTGCCGAAACCTCCTCATAG
Muc2	TCCTGACCAAGAGCGAACAC	ACAGCACGACAGTCTTCAGG
Muc3	CATCTCCCGGAACCTTCCAC	GGCATGTAGTTTTCTCGTTCTTCAT
Muc4	CATCCTCCTCAGGATTGACTACGA	GGGGCTAGTAAGGGTCGAGG
Muc5b	TGATGTTGACCGCTTCCAGG	GACTCATTCACCTGCCGGG
Retnla	GCTGGGATGACTGCTACTGG	CTCCCAAGATCCACAGGCAA
Retnlb	TCAGTCGTCAAGAGCCTAAGAC	GTCTGCCAGAAGACGTGACA
Tff2	GAAACCTTCCCCCTGTCGG	CCAGCGACGCTAGAGTCAAA
Tnf	ATGGCCTCCCTCTCATCAGT	TGGTGGTTTGCTACGACGTG
Tslp	AGGGGCTAAGTTCGAGCAAA	AAGCTGGCTTGCTCTCACAG

Supplemental Experimental Procedures Table 1

Supplemental Figure 1

A

B

C
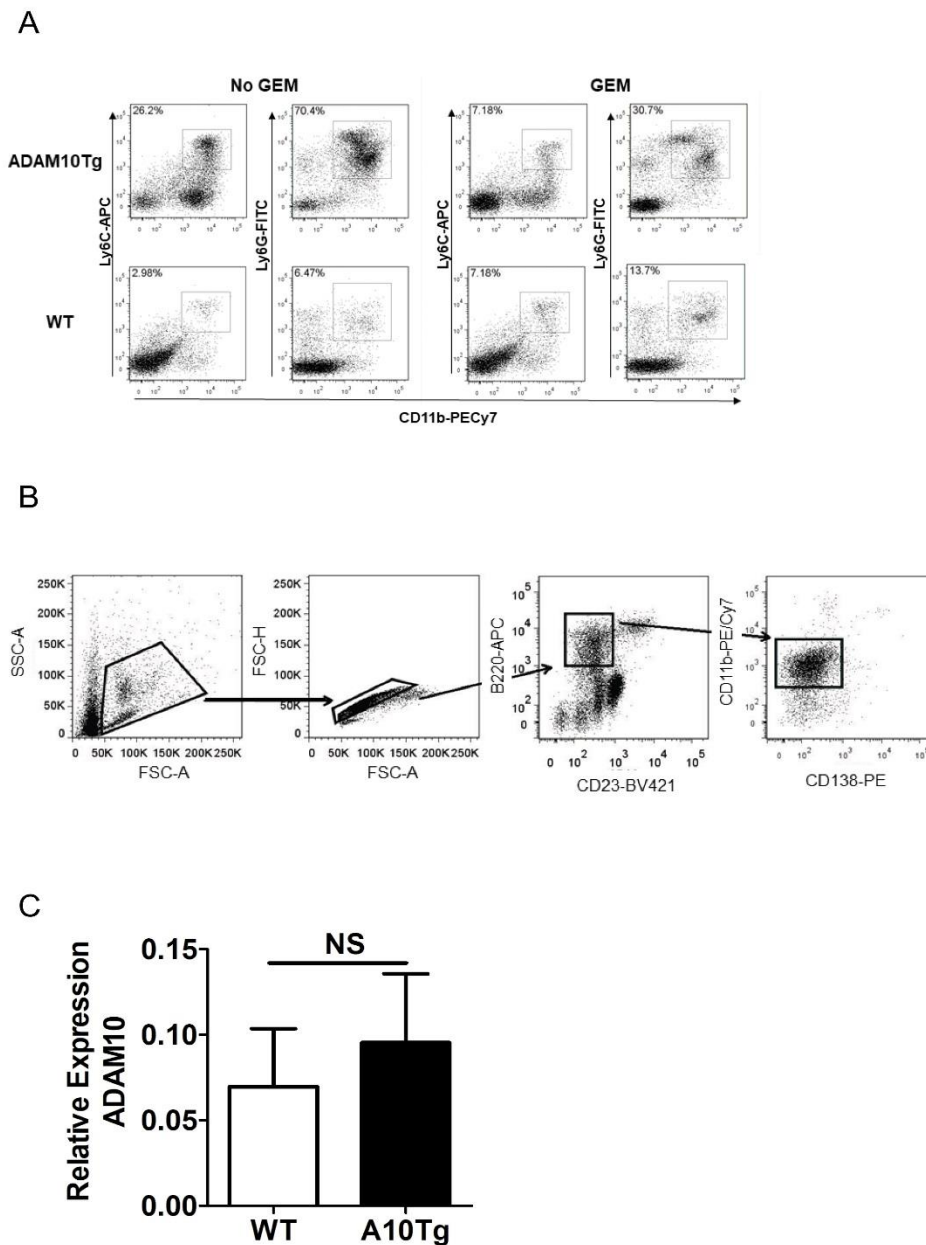
Figure S1. *Adam10* **message is not overexpressed on ADAM10Tg B1 cells, Related to Figure 1**. A. Flow cytometry of spleen from WT and ADAM10Tg (A10Tg) mice infected with *N. brasiliensis,* with and without treatment with gemcitabine (GEM) to deplete MDSCs after 14 days of infection. B1 cells were sorted from the peritoneal lavage (PL) fluid of mice utilizing the gating strategy illustrated in (B). C. *Adam10* message was measured in WT and A10Tg B1 cells from mice infected with *N. brasiliensis*. *Adam10* message is normalized to *Gapdh*. n=4 pooled experiments/group and statistical comparison was performed using a Mann-Whitney non-parametric analysis. NS=not significant. Error bars depict SEM.
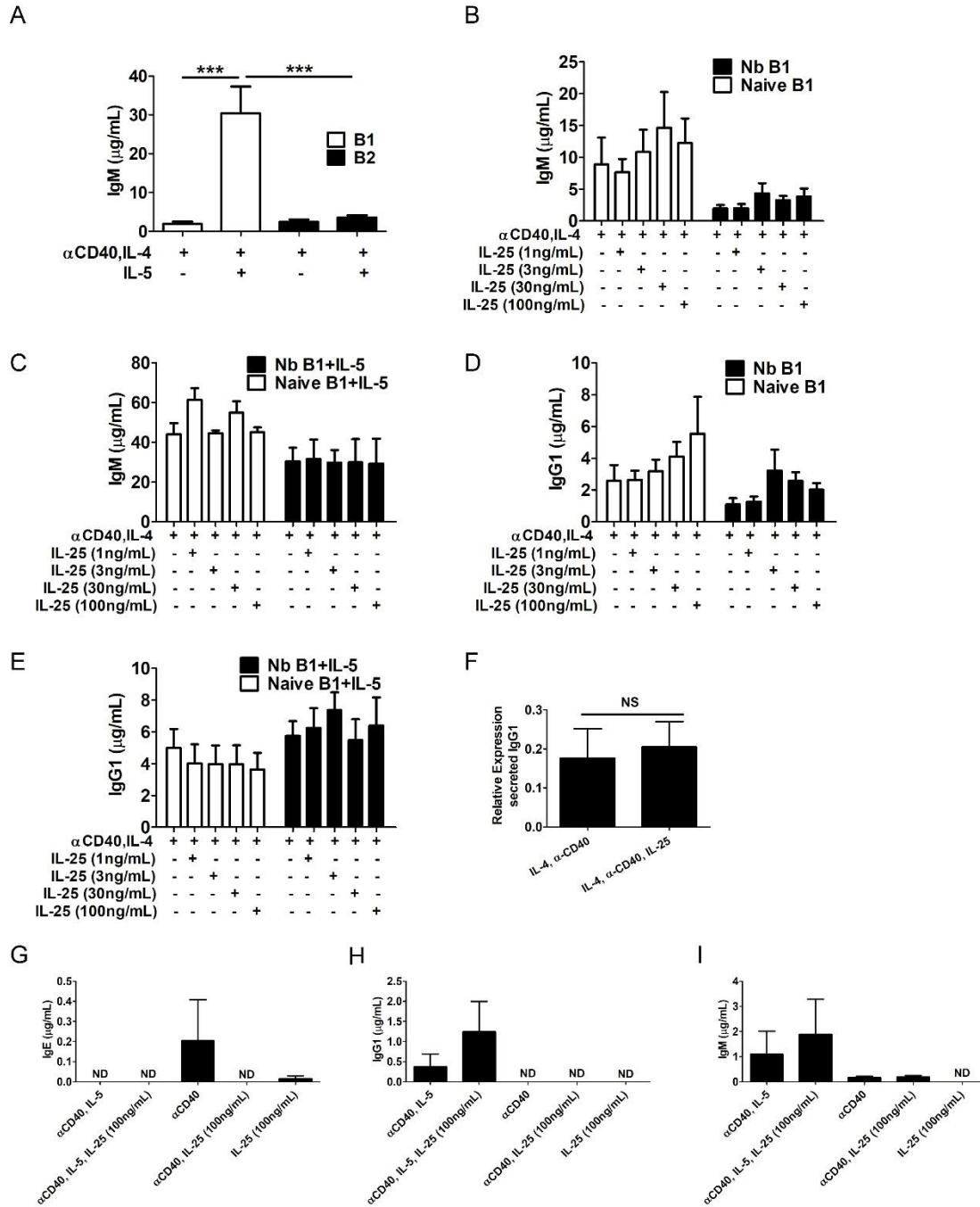
Figure S2. B1 cells from mice infected with *N. brasiliensis* make more IgM in response to IL-5, but not IL-25 Related to Figure 4 and 5. B1 and B2 cells were sorted from mice infected with *N. brasiliensis*(A, B, C, D, E, G, H, I) or naïve (B, C, D, E) and cultured for 9 days with anti-CD40, IL-4, and ± IL-5(A, C, E) and/or ± IL-25(B, C, D, E). Controls are indicated (G, H, I). An ELISA was performed to detect total IgM (A, B, C, I), IgG1 (D, E, H), or IgE (G) in cell-free supernatants. Relative expression of secreted *Ighg1* message (F) was assessed in cells cultured with or without added IL-25 and normalized to *Actb* message. ***p<0.001, NS=not significant. Error bars depict SEM. n>7 mice (A-E) n=3 pooled experiments/group. Statistical comparison was performed using a one-way ANOVA with a Tukey post hoc test.
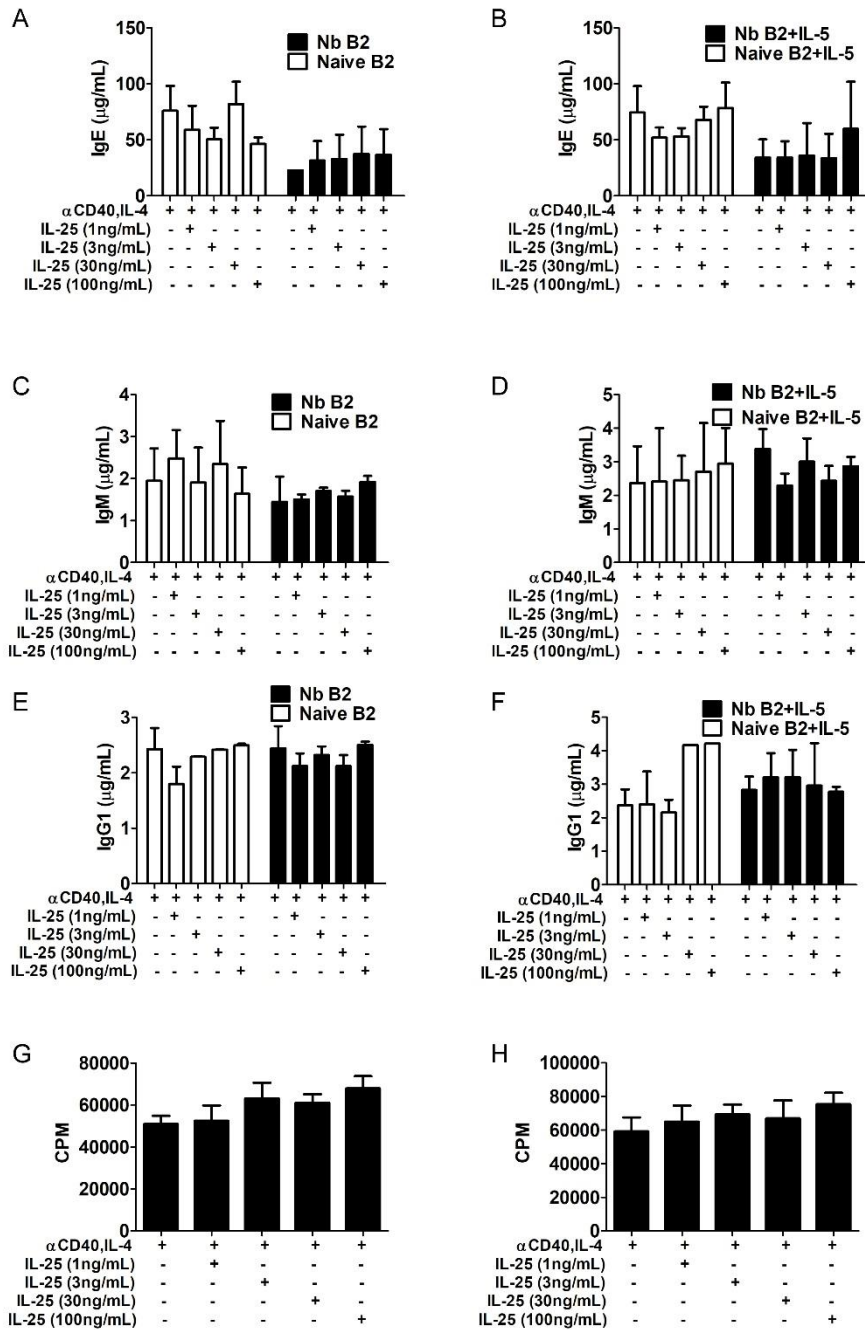
Figure S3. B2 cells from mice infected with *N. brasiliensis* or naïve mice are not induced to proliferate or secrete antibody by IL-25, Related to Figure 5. B2 cells were sorted from the PL of naïve mice or mice infected with *N. brasiliensis* (Nb). They were then cultured with anti-CD40 and IL-4 followed by detection of (A-F) antibody in the cell-free supernatants and (G-H) proliferation. Total IgE, IgM, and IgG1 were measured in the (A,C,E) absence or (B,D,F) presence of IL-5 added to culture respectively. Proliferation was performed as in Figure 5 on B2 cells from mice infected with *N. brasiliensis* with (G) or (H) without IL-5 added to culture. CPM = counts per minute. All cells were treated with increasing doses of IL-25. Error bars depict SEM. n>7 mice per group and statistical analyses used Student's T-test to compare IL-25-treated and non-treated groups. Data are inclusive of three independent experiments.

Supplemental Figure 4
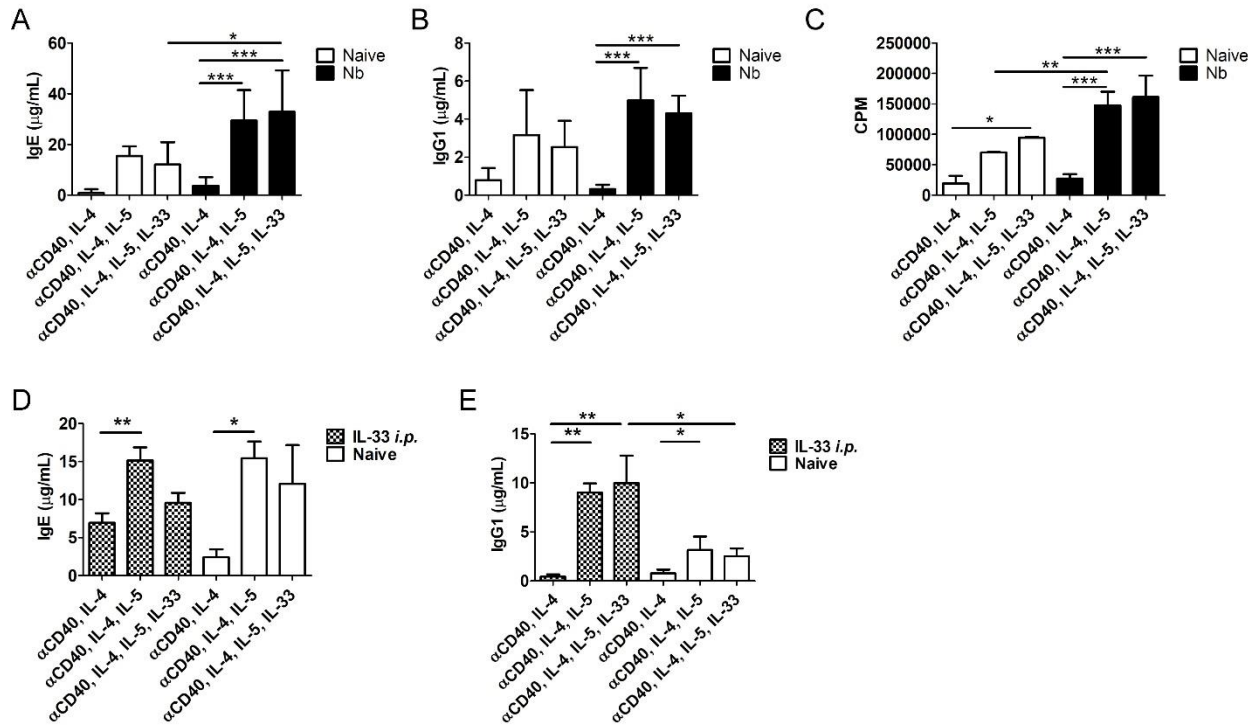
Figure S4. IL-33 does not enhance B1 cell IgE production, Related to Figure 5. B1 cells from naïve mice and mice infected with *N. brasiliensis* (Nb) were sorted and cultured with anti-CD40, IL-4 and ± IL-5 for 48 hours, followed by the addition of IL-33. After 9 days of culture, cell free supernatants were measured for total IgE (A) and IgG1 (B). Cell proliferation was also determined by culturing cells with anti-CD40, IL-4, and ± IL-5 for 48 hours and then adding IL-33. 24 hours later, 1μCi H^3 was added and after 24 hours of incubation the plate was harvested onto GFC plates and read on a TopCount plate reader. CPM = counts per minute. (D,E) Mice were *i.p.* injected with 2μg/mouse IL-33 daily for 7 days and then B1 cells were sorted from both these mice and naïve mice. After 9 days of culture, total IgE (D) and IgG1 (E) was measured. *p<0.05 **p<0.01 ***p<0.001. Error bars depict SEM. Significance was determined with a one-way ANOVA with a Tukey Post-hoc test.

Supplemental Figure 5
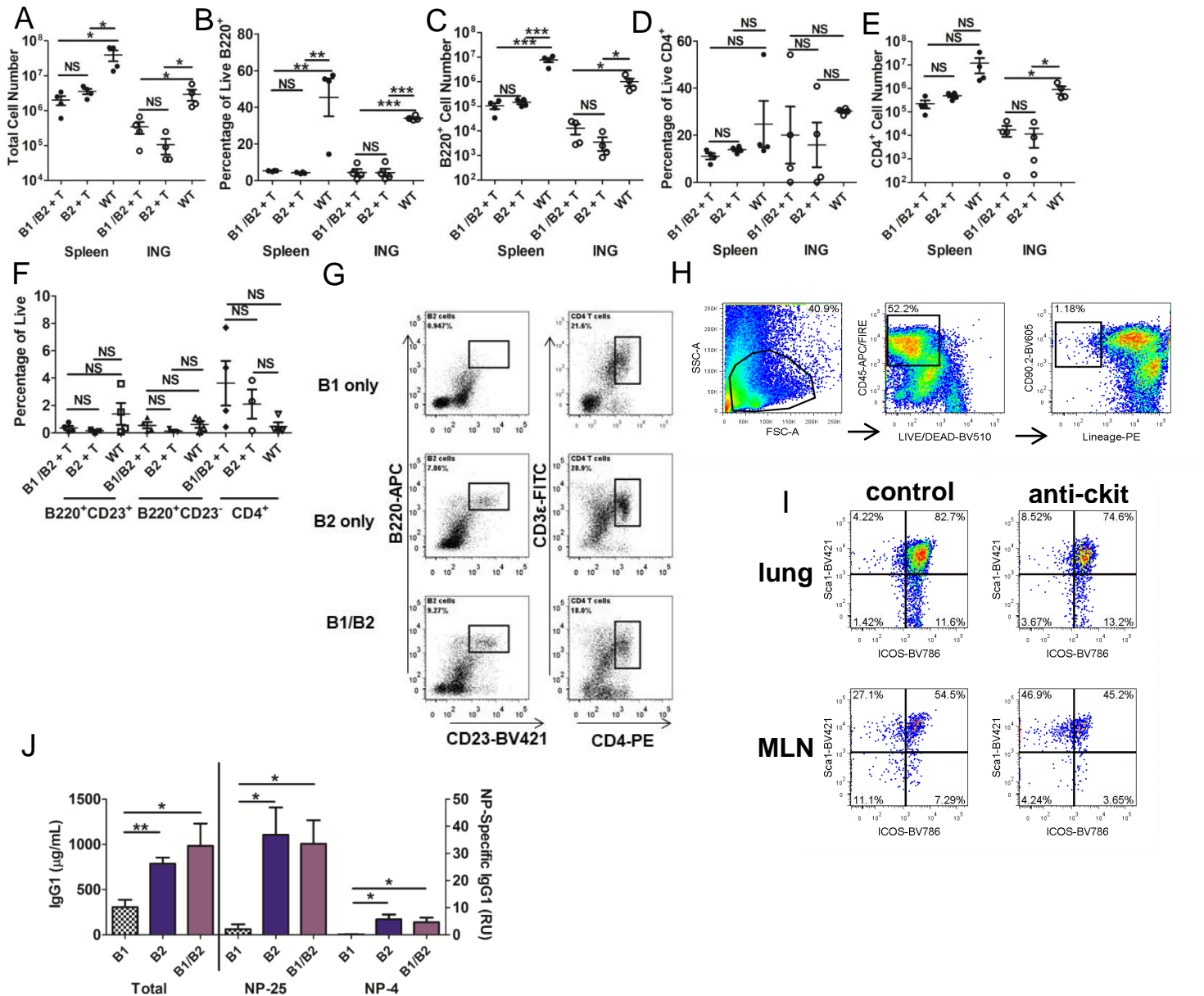
Fig S5. RAG1^{-/-} reconstitution is confirmed by flow cytometry after reconstitution and after infection with *N. brasiliensis*, Related to Figure 6. Flow cytometry was performed on spleen, PL and inguinal lymph node (ING) cells on day 7 after reconstitution A-F, and mesenteric lymph node (MLN) on day 21 after inoculation with *N. brasiliensis* (G). A. Total organ cell counts. B and C are percent and cell number respectively of CD45^{+}B220^{+} cells, and D and E are percent and cell number respectively for CD45^{+}CD4^{+} cells. F is percent of CD45^{+}B220^{+}CD23^{+} (B2) cells, CD45^{+}B220^{+}CD23[-](B1) cells, and CD45^{+}CD4^{+} cells in the PL. G is representative flow on MLNs. H. Gating strategy for ILC2s. I. Representative dot plots for ILC2 determination for Figure 7.G and H from digested lung and MLN. J. RAG1^{-/-} mice were reconstituted as in Figure 6 and then immunized *i.p.* with NP$_{32}$-KLH in alum. High affinity and total NP-specific IgG1 and total IgG1 were measured in the serum by ELISA as described for Fig. 2 on day 14. *p<0.05 **p<0.01 ***p<0.001. Error bars depict SEM. n=4/group for A-F. n>7 mice/group for J. Significance was determined with a one-way ANOVA with a Tukey Post-hoc test.

14

	Relative to *Hprt*					
	B2 + T cell	**T cell Only**	**Rag1^{-/-} No Reconstitution**	**Naive**	**adj. *P value* (B2+T cell vs. naive)**	**adj. *P value* (B2+T cell vs. T cell only)**
Ccl2	0.077044286	0.093739571	0.0112724	0.002798	0.013961	0.682789701
Ccl11	0.153465857	0.061919714	0.026749	0.0208124	0.044843	0.097642131
Chi3l	0.000345614	0.000122967	0.00007804	9.4725E-06	0.020655	0.060076939
Cma1	0.024789571	0.006773714	0.0028904	0.0017496	0.008128	0.014051213
Cpa3	0.068068286	0.016118286	0.0176172	0.0022334	0.003627	0.005956175
Fcer1a	0.156148143	0.022642	0.0082074	0.002693	0.029824	0.021994047
Fcgbp	0.00051315	2.19814E-05	7.61667E-05	0.00002719	0.062147	0.01252311
Il4	0.005076243	0.001648714	0.0003178	0.0001644	0.085558	0.163845777
Il5	0.001869857	0.001792	0.0002637	0.0000891	0.014381	0.933434232
Il6	0.007308714	0.006642571	0.001565	0.0005286	0.049622	0.849245398
Il9	0.066535143	0.024044143	0.006839	0.001173	0.046645	0.121267873
Il13	0.005123557	0.002470429	0.000585	0.0001321	0.016998	0.237206092
Il22	0.000401286	0.00031768	0.0001999	0.000061648	0.036571	0.662990261
Il25	0.188965143	0.084581571	0.0059146	0.0033306	0.096698	0.357499826
Il33	0.009379857	0.011231714	0.0172744	0.0286112	0.145367	0.633328373
Mcpt1	0.126148286	0.035677286	0.1074352	0.007403	0.008382	0.014506206
Mcpt2	0.058289286	0.013659	0.0213562	0.0008854	0.012884	0.018588217
Mcpt4	0.013884571	0.007327143	0.0053466	0.0006952	0.237453	0.485531782
Muc1	0.000447343	2.93287E-05	1.73777E-05	0.00001287	0.144678	0.083333152
Muc2	0.000434243	0.000164141	0.00007188	0.000028702	0.003950	0.054720378
Muc3	0.0001672	0.000006988	0.000033296	1.77245E-05	0.002572	5.6789E-06
Muc4	0.001043	8.83271E-05	0.00010196	0.00005934	0.004945	0.001295176
Muc5b	0.001103667	0.000123857	0.00023918	0.000011478	0.004818	0.000667575
Retnla	0.0014116	0.00025974	0.000126092	0.000009806	0.005520	0.011604179
Retnlb	0.000218638	0.000123653	3.52067E-05	3.33667E-05	0.318206	0.587769427
Tff2	0.003614357	0.000299714	0.00013786	0.000128708	0.015806	0.006160113
Tnf	0.03976	0.007283286	0.0025956	0.0013356	0.061868	0.058523604
Tslp	0.001196167	0.0004902	0.000080648	9.8725E-06	0.015849	0.115030279
Ccl24	0.209496667	0.213941429	0.0592898	0.0291746	0.033112	0.033112
Chi3l4	0.004223967	0.00273828	0.090120876	0.0060115	0.762824	0.7628241
Ear11	0.086239286	0.160493429	0.001719	0.20005054	0.522387	0.5223871
Epx	0.001855167	0.001147514	0.000125988	0.000215382	0.021077	0.021077
Gsdmc2	0.336043667	0.491415714	0.1833276	0.0666722	0.098321	0.098321
Il10	0.000395486	0.000210367	0.0016544	0.00007306	0.101834	0.1018343
Mcpt8	0.000337714	0.0000967	0.00009954	0.0000357	0.082365	0.082365
Prg2	0.042052571	0.025133143	0.0048764	0.0054274	0.036326	0.036326
Timp1	0.034064	0.074320429	0.0069508	0.0030494	0.042338	0.0423376

Table S1. Intestinal gene expression in naïve or *N. brasiliensis* infected RAG1^{-/-} mice, with or without reconstitution, Related to Figure 7. Genes are expressed relative to housekeeping *Hprt*.

	Relative to *Hprt*		
	B2 + T cell	**T cell Only**	**adj. *P value* (B2 + T cell vs. T cell only)**
Ccl11	0.03783	0.0328	>0.9999
Chi3l	33.38	34.87	>0.9999
Cpa3	8.908	9.038	>0.9999
Ear11	216.6	104.4	0.0292
Epx	0.3414	0.4475	>0.9999
Fcer1a	0.02022	0.01704	>0.9999
Il4	98.8	52.02	>0.9999
Il5	95.86	62.38	>0.9999
Il6	0.01726	0.008323	>0.9999
Il13	6.823	4.109	>0.9999
Il33	7.748	3.262	>0.9999
Mcpt1	0.4091	0.3219	>0.9999
Mcpt2	1.306	0.478	>0.9999
Mcpt4	3.253	1.995	>0.9999
Mcpt8	241.6	215	>0.9999
Muc5ac	1.157	1.318	>0.9999
Retnla	3.839	1.586	>0.9999
Retnlb	0.03805	0.03035	>0.9999
Tnf	0.4493	1.377	>0.9999
Tslp	0.4284	0.3338	>0.9999

Table S2. Lung gene expression in *N. brasiliensis* infected RAG1^{-/-} mice. Related to Figure 7. Genes are expressed relative to housekeeping *Hprt*.